

Metamorphism of Mafic Rocks

9



Kyanite-eclogite from Verpeneset, Nordfjord, Norway. Omphacite (green), garnet (red brown, zoned) are the main minerals, additional minerals include kyanite, zoisite and phengite. The rock formed by Caledonian high-pressure metamorphism.

9.1 Mafic Rocks

Metamorphic mafic rocks (e.g. mafic schist or greenschist and mafic gneiss, amphibolite, mafic granulite) are derived from mafic igneous rocks, mainly basalt and andesite, and of lesser importance, gabbro and mafic diorite (Chap. 2; Fig. 9.1). Metamorphic assemblages in mafic rocks are particularly useful in defining the intensity of metamorphism within the metamorphic facies concept (Chap. 4).

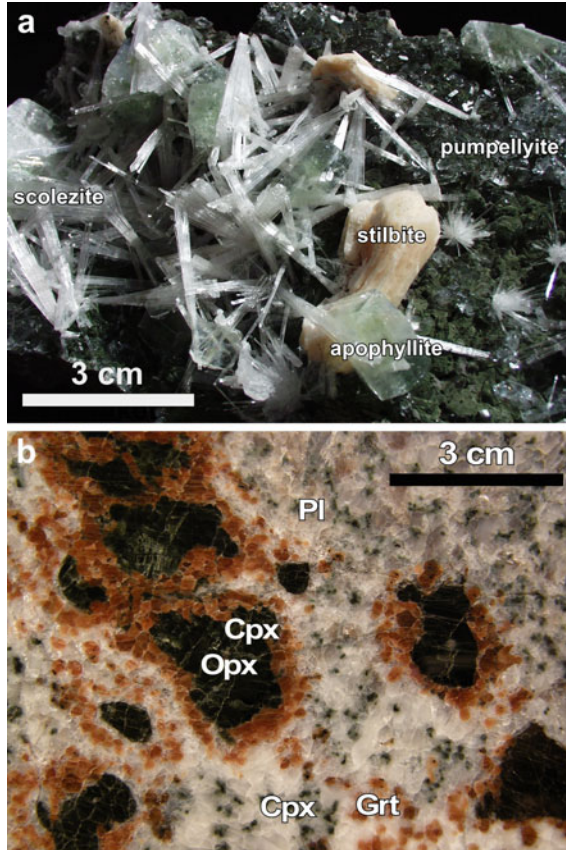


Fig. 9.1 **a** Low temperature minerals precipitated from hydrothermal fluid cover basaltic volcanic rocks at Poona (India). A continuous thin layer of dark green pumpellyite covers the basaltic rock. On this early reaction product younger (and at lower T) Ca-zeolites scolezcite and stilbite crystallized from thermal water together with apophyllite. **b** Granulite facies troctolite from Holsnøy (Bergen Arcs, Norway). Rock matrix contains predominantly plagioclase and fine grained Cpx and Grt. Large coronitic structures with occasionally Opx in the core, rimmed by dark Cpx and a corona of coarser grained clear garnet replaced igneous olivine megacrysts. The igneous assemblage Ol + Pl has been replaced by the Grt + Cpx + Pl granulite assemblage. Note that there is also fine-grained Cpx and Grt in the Pl-matrix of the rock

Extrusive mafic igneous rocks comprise the largest volume of mafic rocks in comparison to their plutonic equivalents (Tables 2.1 and 2.2). Basalts and andesites occur as massive lava flows, pillow lavas, sills, dykes, hyaloclastic breccias and tuff layers (Figs. 9.2 and 9.3). Basaltic rocks constitute a major portion of the oceanic crust and most basalts appear to have been subjected to ocean-floor metamorphism immediately after formation at a spreading ridge. When transported to a continental margin via plate motion, oceanic mafic rocks are again recrystallized at or near convergent plate junctions and are typically retained as fragments within the subduction complex; the change in mineralogy depends on whether the oceanic crust was subducted beneath a continental plate or was obducted onto continental crust. On the other hand, andesitic rocks and related calc-alkaline volcanics together with associated volcanogenic sediments (e.g. typically greywacke) are the dominant lithologies within island arcs and Pacific-type continental margins. These rocks are subjected to alteration by hydrothermal fluids as evidenced by present-day geothermal activity in many island arc areas or are transformed during burial and orogenic metamorphism.

Metamorphosed mafic rocks are particularly susceptible to changes in T and P and this is the main reason why most names of individual metamorphic facies are derived from mineral assemblages of this rock group, e.g. greenschist, amphibolite, granulite, blueschist, and eclogite (cf. Chaps. 2 and 4). In addition, mafic rocks that are metamorphosed under very weak conditions below greenschist and blueschist facies grade often show systematic variations in mineralogy that permits a further subdivision into characteristic metamorphic zones. These distinct low-grade zones have been given separate metamorphic facies names such as zeolite, prehnite-pumpellyite and pumpellyite-actinolite, that are here simply grouped as subgreenschist facies for very-low grade conditions of incipient metamorphism (Fig. 9.1a).

9.1.1 Hydration of Mafic Rocks

Basalts and gabbros have solidus temperatures of about 1200 °C. Consequently, hydrous minerals are not typical members of the solidus assemblage of basalts and other mafic rocks. Therefore, at the onset of metamorphism, mafic rocks, including pyroclastic rocks, are in their least hydrated state as opposed to “wet” sedimentary rocks that start metamorphism in a maximum hydrated state. Because newly formed minerals in metamafic rocks at low- T are predominantly hydrous phases, access of water is essential to initiate metamorphism, otherwise, igneous rocks would persist relatively unchanged in metamorphic terrains. Partial or complete hydration of mafic rocks may occur during ocean-floor metamorphism (Fig. 9.1a), with hydrothermal activity in island arc settings, or during orogenic metamorphism where deformation facilitates the influx of water. During metamorphism of mafic rocks the condition $P_{\text{tot}} = P_{\text{H}_2\text{O}}$ may not be maintained continuously during their prograde reaction history. On the other hand, mafic rocks in many metamorphic terranes show that partial persistence of igneous minerals and microstructures is common in subgreenschist facies rocks and that such features are typically absent in

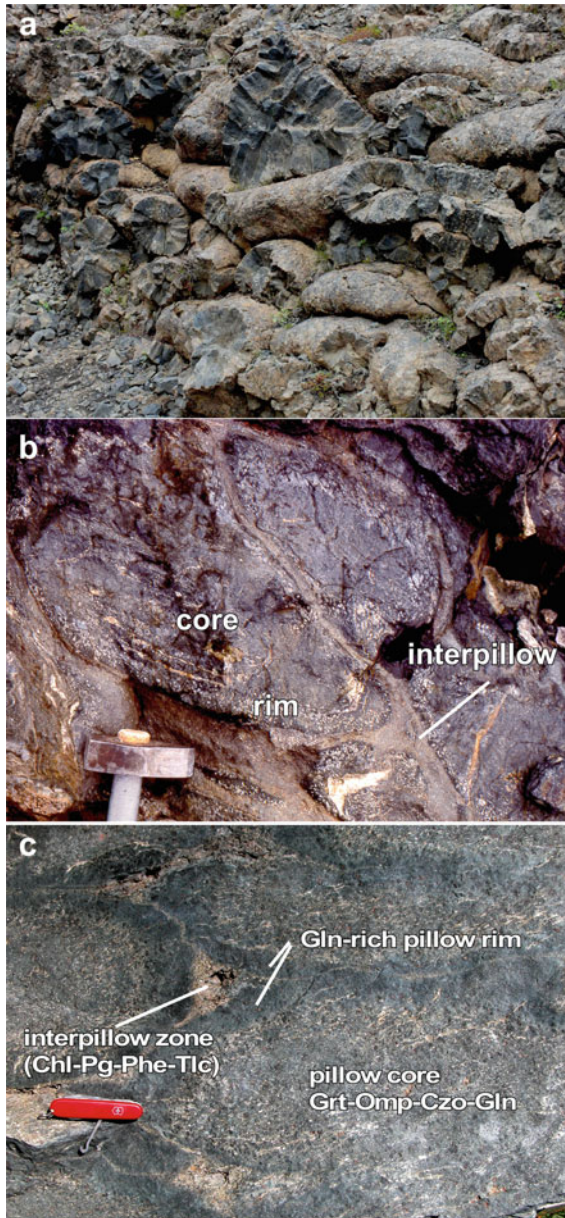


Fig. 9.2 Pillow lava: **a** Young subglacial pillow lava together with palagonite a brownish alteration product of volcanic glass (3 m vertical outcrop; Laugarvatnshellir, Iceland). **b** Small pillows in amphibolite at Muretto Pass (Bergell, Italy). Pillow basalt metamorphosed in the contact aureole of the Tertiary Bergell granitoid intrusion. The rock consists predominantly of plagioclase + hornblende. **c** Eclogite facies basaltic pillow lava from Pfulwe (Zermatt, Alps). Pillow cores contain Grt-Omp + Ep/Czo-Gln-Cld, dark pillow rims contain Gln-Cld-Grt-Omp and minor Czo-Pg-Tlc, interpillow zones are rich in Chl-Pg-Phe and Tlc (Bucher et al. 2005). The compositional zoning probably resulted from seafloor metasomatism



Fig. 9.3 Eclogite facies metabasalt from the Saas valley (Western Alps) with Grt–Omp–Gln–Czo/Ep–Ank–Cld. The rock is typical of fast subduction of oceanic lithosphere ($\sim 7^\circ\text{C km}^{-1}$ geothermal gradient). The rock reached ~ 100 km depth (2.7 GPa) at a very low temperature of only 600°C

rocks metamorphosed to conditions of greenschist facies and higher. Nevertheless, primary igneous meso-structures such as magmatic layering and pillow structures may be preserved even in eclogite and granulite facies terrains (Fig. 9.3a). Coarse-grained gabbroic rocks have the best chance to retain primary igneous minerals up to high-grade metamorphic conditions. Gabbro bodies often escape pervasive internal deformation and this, in turn, prevents access of water, hampers recrystallization and hinders hydration of the igneous minerals.

As pointed out in Chap. 3, dehydration reactions are strongly endothermic. Consequently, hydration of basalt is exothermic and releases large amounts of heat. The heat of reaction released by replacing a basalt assemblage $\text{Cpx} + \text{Pl}$ by low- T hydrous minerals such as $\text{Prh} + \text{Chl} + \text{zeolites}$ could raise the temperature by as much as 100°C (in a heat-conserving system). Another interesting aspect of exothermic reactions is their self-accelerating and feedback nature. Once initiated, they will proceed as long as water is available. Increasing temperature will initially make the reactions go faster, but it will also bring a reaction closer to its equilibrium where it would eventually stop. Also, note that reactions that partially or completely hydrate mafic rocks are metastable reactions and as such tend to run far from equilibrium. Consider, for instance, the reaction $\text{Di} + \text{An} + \text{H}_2\text{O} \rightleftharpoons \text{Chl} + \text{Prh} \pm \text{Qtz}$ mentioned above. In the presence of water at low- T , this reaction will always run to completion and the product and reactant assemblage will never attain reaction equilibrium. Thus, the unstable or metastable nature of the hydration reactions that replace high- T anhydrous igneous assemblages by low- T hydrate assemblages has the consequence that low-grade mafic rocks often show

disequilibrium assemblages. Unreacted high- T igneous assemblages may occur together with various generations of low- T assemblages in subgreenschist facies rocks. The hydration process commonly leads to the development of zoned metasomatic structures, e.g. networks of veins and concentric shells of mineral zones that reflect progressive hydration of basaltic pillow lavas. In this case, the highly permeable inter-pillow zones serve as water-conducting structures for hydration water and the hydration process progresses towards the pillow centers (Figs. 9.2, 9.3 and 9.4a). The nature of the product assemblages depends on the P and T during the hydration process but also on the chemical composition of the hydration fluid. CO_2 in the fluid plays a particularly important role. CO_2 -rich aqueous fluids may result in altered basalts with modally abundant carbonates such as Cal and Ank. CO_2 -rich fluids also tend to favor the formation of less hydrous assemblages compared with pure H_2O fluids. The cation composition of aqueous fluids that have already reacted with large volumes of basalt is drastically different from that of seawater. Fluid that moves rapidly through permeable fractured rocks will have a different composition than fluid that moves slowly through porous basalt. Fluid-rock interaction typically also leads to extensive redistribution of chemical elements, such as in piles of basaltic pillow lavas. Mineralogical evidence for this may still be observed in high-grade metabasaltic rocks. For example, in the Saas-Zermatt ophiolite complex of the Central Alps, Switzerland, mesoscopic pillow lava structures are often preserved with pillow cores of 2.5 GPa eclogite and inter-pillow material of nearly monomineralic Gln (Fig. 9.3a). Finally, the alteration products of the fluid-basalt interaction process will, of course, reflect these compositional differences of the hydration fluid.

A heterogeneous degree of hydration also results in features such as incipient to extensive development, sporadic distribution, and selective growth of low-grade minerals in vesicles and fractures (Fig. 9.4b), and the topotaxial growth of these minerals after igneous Pl, Cpx, Ol, Hbl, Fe-Ti oxides, and glass. From the viewpoint of the igneous petrologist, these minerals are usually referred to as “secondary or deuteric minerals”. Depending on the effective bulk composition of local domains of a mafic rock, different associations of secondary minerals may develop in vesicles, veins and patches replacing primary phases very irregularly even on the scale of a single thin section. Furthermore, relic igneous phases such as Pl and Cpx and their preserved textural relations are common (e.g. ophitic textures). These igneous anhydrous phases may still form the stable assemblage at low- T under water-absent conditions (Fig. 9.4b). From the viewpoint of the metamorphic geologist, the low-grade hydrates and carbonates, the “secondary or deuteric minerals”, constitute the stable low-grade assemblage under water-present conditions and the starting material of prograde metamorphism (Fig. 9.1a). In the conceptually simplest case, no relic igneous minerals remain in the mafic rock and its igneous assemblage has been completely replaced by a stable low- T assemblage and the rock is in its maximum hydrated state at low- T (Fig. 9.4a).

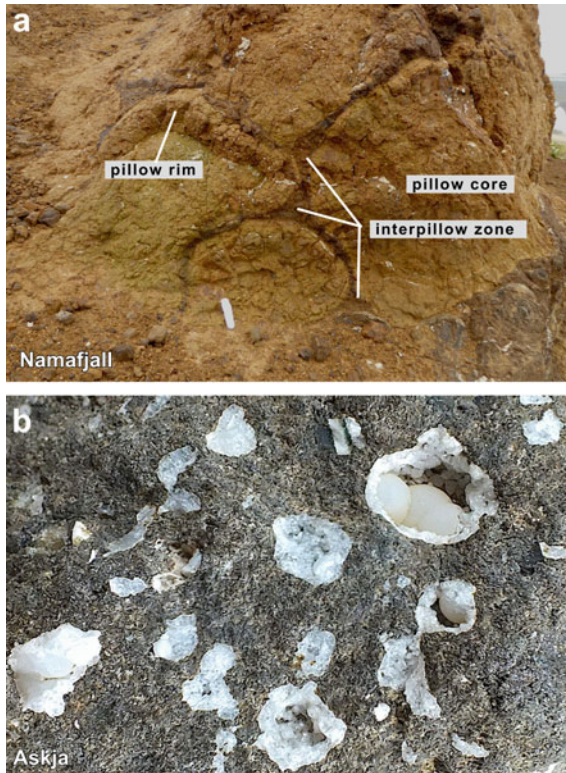


Fig. 9.4 **a** Palagonite outcrop at Namafjall, Iceland. Palagonite is an alteration and partial hydration product of volcanic glass (hydrated hyaloclastite) and but also, as shown on the photograph, of pillow basalt. The interaction of the basalt with hydrothermal fluids produces hydrous minerals including different clay minerals such as illite, kaolinite and smectite and various zeolites. **b** Vesicular basalt with small cavities partially filled with zeolite minerals, here mesolite and scolecite. Size of vesicles about 5–10 mm (Breiðdal, Iceland)

9.1.2 Chemical and Mineralogical Composition of Mafic Rocks

The characteristic composition of alkali-olivine basalt is listed in Table 2.1 and of a mid-ocean ridge basalt (MORB) in Table 2.3. MORB that is produced along ocean spreading centers is by far the most common type of mafic rock and will serve as a reference composition for all mafic rocks discussed in this chapter. Mafic rocks are characterized by SiO_2 contents of about 45–60 wt.% and are also relatively rich in MgO, FeO, CaO and Al_2O_3 . It is general custom in petrology to term igneous rocks with 45–52 wt.% SiO_2 *basic*, and their metamorphic derivatives are then called metabasic or metabasaltic rocks, in short, metabasites. Andesitic rocks, on the other hand, contain higher SiO_2 , Al_2O_3 , and alkalis, but lower MgO, FeO, and CaO than

basalts (e.g. Carmichael 1989); basaltic andesites and andesites belong to the *intermediate* igneous rocks, defined by SiO_2 contents of 52–63 wt.%.

Basic or mafic igneous rocks contain appreciable amounts of at least the following eight oxide components: SiO_2 , TiO_2 , Al_2O_3 , Fe_2O_3 , FeO , MgO , CaO , Na_2O , with K_2O , MnO , P_2O_5 , H_2O , and CO_2 also present in small amounts. These components are stored in relatively few minerals. The mineral inventory of the mafic protolith comprises the major constituents Pl and Cpx. In addition, Qtz, Opx, Ol and Ne can be present in various associations with Cpx + Pl. Plagioclase and Cpx are the most common minerals of most mafic rocks and many gabbros and basalts contain more than 90–95 vol.% of these minerals. Other basalts and gabbros may be composed of Pl + Cpx + Opx + Qtz or Pl + Cpx + Ol + Ne, troctolites contain Pl + Ol, anorthosites have more than 90 vol.% Pl, etc. However, all mafic rocks are always combinations of only a few mineral species. A large variety of minor and accessory minerals including Ilm, Mag, Chr, sulphides, Grt, Ap, carbonate, and even Hbl and Bt can also occur in mafic rocks. The later two hydrous minerals are often poor in OH as a result of oxidation and/or halogen substitution.

The complex chemical bulk rock composition of basalts will be redistributed from the few igneous mineral species into a variety of new minerals during metamorphism. The high CaO content of the chief basalt minerals Cpx and Pl results in the formation of numerous separate calcium-bearing metamorphic minerals such as Prh, Pmp, Ttn, Ep, Pl, Am and Grt. This is the essential difference from metapelitic rocks (Chap. 7) where CaO is very low and does not form separate calcic phases but rather occurs as a minor component in ordinary Fe–Mg minerals such as garnet. The most important minerals found in metamafic rocks are listed in Table 9.1.

9.1.3 Chemographic Relationships and ACF Projection

The composition space that must be considered in an analysis of phase relationships in metamafic rocks is rather complex and requires eight or more system components. This follows from above and from the chemical analysis of MORB in Table 2.2. A graphical analysis of phase relationships in metamafic rocks is often made by means of the ACF projection, the principles of which were introduced in Sect. 2.5.3 and shown in Figs. 2.15 and 2.16. In general, the ACF diagram is used for the representation and analysis of phase relationships that involve calcic minerals. Because of its importance for the subsequent treatment of metamafic rocks some important features of the ACF projection are briefly reviewed.

The following discussion makes extensive use of Fig. 9.5a that is a pseudo-3D display of the NACF tetrahedron, and Fig. 9.5b, a conventional ACF diagram. The ACF diagram represents a mole fraction triangle and displays the three composition variables Al_2O_3 , CaO and FeO . Any mineral that is composed of only these three components can be directly shown on an ACF diagram (e.g. hercynite). Any other mineral composition is projected onto the ACF triangle or is used as a projection point. In the latter case, the mineral must be present in all assemblages in order to

Table. 9.1 Minerals in metabasaltic rocks

<i>Nesosilicates</i>	
Garnet	$(\text{Fe}, \text{Mg}, \text{Ca})_3(\text{Al}, \text{Fe})_2\text{Si}_3\text{O}_{12}$
<i>Sorosilicates</i>	
Kyanite	Al_2SiO_5
Zoisite	$\text{Ca}_2\text{Al}_3\text{Si}_3\text{O}_{12}(\text{OH})$
Epidote	$\text{Ca}_2\text{FeAl}_2\text{Si}_3\text{O}_{12}(\text{OH})$
Pumpellyite	$\text{Ca}_4\text{Mg}_1\text{Al}_5\text{Si}_6\text{O}_{23}(\text{OH})_3 \cdot 2 \text{H}_2\text{O}$
Vesuvianite	$\text{Ca}_{19}\text{Mg}_2\text{Al}_{11}\text{Si}_{18}\text{O}_{69}(\text{OH})_9$
Lawsonite	$\text{CaAl}_2\text{Si}_2\text{O}_7(\text{OH})_2 \cdot \text{H}_2\text{O}$
Chloritoid	$\text{Mg}_1\text{Al}_2\text{Si}_1\text{O}_5(\text{OH})_2$
<i>Pyroxenes</i>	
Diopside	$\text{CaMgSi}_2\text{O}_6$
Jadeite	$\text{NaAlSi}_2\text{O}_6$
Hypersthene	$(\text{Mg}, \text{Fe})_2\text{Si}_2\text{O}_6$
Omphacite	$(\text{Ca}, \text{Na})(\text{Mg}, \text{Fe}, \text{Al})\text{Si}_2\text{O}_6$
<i>Amphiboles</i>	
Tremolite	$\text{Ca}_2\text{Mg}_5\text{Si}_8\text{O}_{22}(\text{OH})_2$
Actinolite	$\text{Ca}_2(\text{Fe}, \text{Mg})_5\text{Si}_8\text{O}_{22}(\text{OH})_2$
Glaucophane	$\text{Na}_2(\text{Fe}, \text{Mg})_3(\text{Al})_2\text{Si}_8\text{O}_{22}(\text{OH})_2$
Barroisite	$(\text{Ca}, \text{Na})_2(\text{Fe}, \text{Mg}, \text{Al})_5\text{Si}_8\text{O}_{22}(\text{OH})_2$
Tschemmakite	$\text{Ca}_2(\text{Fe}, \text{Mg})_3(\text{Al})_2(\text{Al}_2\text{Si}_6\text{O}_{22}(\text{OH})_2)$
Hornblende	$(\text{Na}, \text{K})\text{Ca}_2(\text{Fe}, \text{Mg}, \text{Al})_5(\text{Si}, \text{Al})_8\text{O}_{22}(\text{OH}, \text{F}, \text{Cl})_2$
<i>Sheet silicates</i>	
Muscovite	$\text{KAl}_3\text{Si}_3\text{O}_{10}(\text{OH})_2$
Celadonite	$\text{KMgAlSi}_4\text{O}_{10}(\text{OH})_2$
Paragonite	$\text{NaAl}_3\text{Si}_3\text{O}_{10}(\text{OH})_2$
Phlogopite	$\text{KMg}_3[\text{AlSi}_3\text{O}_{10}](\text{OH})_2$
Biotite	$\text{K}(\text{Mg}, \text{Fe}, \text{Al}, \text{Ti})_3[(\text{Al}, \text{Si})_3\text{O}_{10}](\text{OH}, \text{F}, \text{Cl})_2$
Clinochlore	$\text{Mg}_5\text{Al}_2\text{Si}_3\text{O}_{10}(\text{OH})_8$
Chlorite	$(\text{Fe}, \text{Mg})_5\text{Al}_2\text{Si}_3\text{O}_{10}(\text{OH})_8$
Prehnite	$\text{Ca}_2\text{Al}_2\text{Si}_3\text{O}_{10}(\text{OH})_2$
<i>Tectosilicates</i>	
Quartz	SiO_2
Anorthite	$\text{CaAl}_2\text{Si}_2\text{O}_8$
Albite	$\text{NaAlSi}_3\text{O}_8$
Analcite	$\text{NaAlSi}_2\text{O}_6 \cdot \text{H}_2\text{O}$
Scapolite	$\text{Ca}_4(\text{Al}_2\text{Si}_2\text{O}_8)_3(\text{CO}_3, \text{SO}_4, \text{Cl}_2)$
<i>Zeolites</i>	
Stilbite	$\text{CaAl}_2\text{Si}_7\text{O}_{18} \cdot 7 \text{H}_2\text{O}$
Heulandite	$\text{CaAl}_2\text{Si}_7\text{O}_{18} \cdot 6 \text{H}_2\text{O}$
Laumontite	$\text{CaAl}_2\text{Si}_4\text{O}_{12} \cdot 4 \text{H}_2\text{O}$

(continued)

Table. 9.1 (continued)

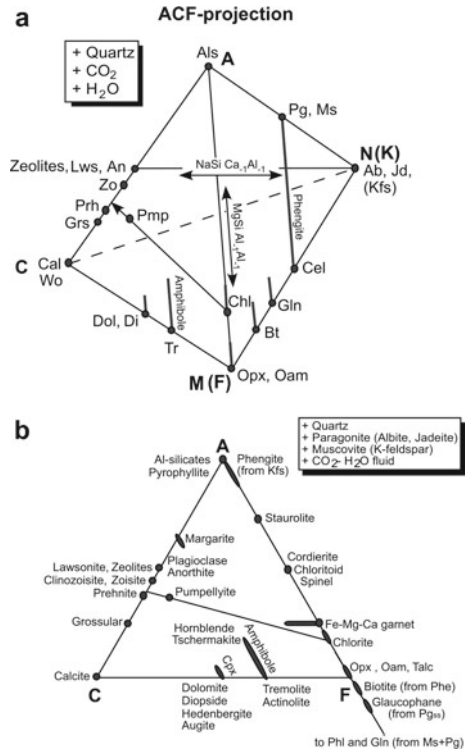
<i>Nesosilicates</i>	
Wairakite	$\text{CaAl}_2\text{Si}_4\text{O}_{12} \cdot 2 \text{H}_2\text{O}$
<i>Carbonates</i>	
Calcite	CaCO_3
Aragonite	CaCO_3
Dolomite	$\text{Ca}(\text{Mg, Fe})(\text{CO}_3)_2$

deduce meaningful phase relationships. As ACF diagrams are projections from SiO_2 . This means that at any given P – T the stable polymorph of SiO_2 (e.g. Qtz) must be present in all assemblages. This restriction often causes a problem when dealing with metamorphic silica-poor igneous mafic rocks such as troctolite, olivine gabbro, olivine basalt and nepheline basalt. However, other meaningful diagrams may be designed for such quartz-free metamafic rocks following the suggestions given in Sect. 2.5. ACF diagrams are also projections from H_2O and CO_2 in order to permit the display of hydrous and carbonate minerals. This means that a fluid phase of a specified composition must be present, or the chemical potentials of H_2O and CO_2 must be defined. This again may cause problems, particularly at low metamorphic grades, because the universal presence of a fluid phase is not obvious in anhydrous igneous protolith rocks (see discussion above). Note also that Pmp plots on the ACF surface in Fig. 9.5a and its composition projects between Zo and Prh as viewed from the Mg-Chl (clinocllore) composition. Note the exchange directions for plagioclase ($\text{Na Si Ca}_1 \text{Al}_1$) and the tschermak substitution ($\text{Mg Si Al}_1 \text{Al}_1$) can be displayed on Fig. 9.5a. The minerals Cpx (Di), Ca-amphibole, Opx, Chl, Phe (Ms-Cel), Na-amphibole and Bt show Tschermak variation on Fig. 9.5a, which is parallel to the Tschermak exchange vector.

ACF diagrams also represent projections parallel to the MgFe_{-1} exchange vector. This is a rigid and lamentable feature of ACF diagrams. All complex relationships, continuous and discontinuous reactions arising from variations in the Fe–Mg ratio of Fe–Mg silicate minerals cannot be properly analyzed and understood with the aid of such diagrams. The AF binary is reduced to a point on ACF diagrams. However, many of the relationships discussed in Chap. 7 with respect to metapelites are also valid here. In Chap. 7 the AF binary is expanded to the AFM triangle and in order to include Ca-minerals AF is reduced to a point in the ACF triangle of this chapter. Although an ACFM tetrahedron would permit a rather thorough analysis of phase relationships in metamafic rocks, it is very inconvenient to work with three-dimensional composition phase diagrams on 2D-surfaces.

The MgFe_{-1} projection on ACF diagrams has the consequence that crossing tie-line relationships among Fe–Mg silicates (with contrasting X_{Fe}) and Ca-minerals do not necessarily represent a discontinuous reaction relationship but rather span a composition volume in the ACFM space. For example (Fig. 9.5b), the presence of four minerals Grt, Hbl, Ky, and Zo can be related to the reaction, $2 \text{Ts} + 1 \text{Ky} = 2 \text{Grt} + 2 \text{Zo} + 1 \text{Qtz} + 1 \text{H}_2\text{O}$. This important reaction in high- P amphibolites is not discontinuous, as may be concluded erroneously from Fig. 9.5b. The four minerals

Fig. 9.5 Composition space and diagrams for metamorphic mafic rocks: **a** Pseudo-3D NACF diagram with plagioclase and tschermak exchange directions and FM (FeMg^{-1}) reduced to a single point. **b** Representation of mineral compositions on an extended ACF diagram



actually occupy corners of a composition volume in ACFM space and may occur as a stable assemblage over a certain $P-T$ interval. The reaction formulated above is thus a continuous reaction. Another effect of the MgFe_{-1} projection is that Fe- and Mg-endmembers of a given mineral species project to identical positions (and of course any intermediate X_{Fe} composition of that mineral as well, e.g. Prp and Alm garnet). The consequences of the MgFe_{-1} projection on ACF diagrams must always be kept in mind.

About 3 wt.% of Na_2O is present in typical basalts (Table 2.3) and Na-bearing minerals such as Pl, Na-Am, Na-Cpx and Na-mica, can be important in metamafic rocks. If one wants to represent sodic phases on ACF diagrams, the ACF triangle must be expanded to a tetrahedron with NaAlO_2 as an additional apex (Fig. 9.5a). At this apex plot the compositions of Ab, Jd and Anl (Qtz, H_2O projection). In a similar fashion, Kfs will plot at the KAIO_2 apex of an analogous K-tetrahedron. Endmember Pg and Ms project onto the AN and AK binary, respectively. All Pl compositions project onto the ACN ternary as the compositional variation of Pl is mainly related to the $\text{NaSiAl}_1\text{Ca}_1$ exchange that relates Ab and An in Fig. 9.5a. The same exchange component can also be found in, for example, Am, Cpx and Mrg. End member Cel, Gln and Phl (Bt) project onto the MN- and MK binary, respectively. The micas and amphiboles also show strong $P-T$ —and assemblage-

dependent compositional variations along the $\text{MgSiAl}_1\text{Al}_1$ -exchange direction. This Ts-exchange is parallel to the AM-(AF)binary. Phengite projects onto the AMN—(AFN) ternary and the solid solution series connects Ms and Cel. Sodic phases are often depicted on ACF diagrams by projecting from the NaAlO_2 apex of the ACFN tetrahedron onto the ACF triangle. This means that Ab, Jd, Anl (whatever is stable at the P and T of the diagram) is present as an extra mineral or that the chemical potentials of these phase components are fixed. It can be seen in Fig. 9.5a that Ab cannot be shown on ACF diagrams and that any Ca-bearing plagioclase will plot at the An position. This means that the consequences of the Pl composition on phase relationships in metamafic rocks cannot be analyzed on ACF diagrams. Muscovite and Pg will project to the A apex of ACF diagrams, whereas Phe occupies the entire AF-binary when projected from Kfs (Ab). However, as Kfs is very rare in metamafic rocks, Kfs projections are not commonly used. In analogy to AFM diagrams, one may project from the white micas rather than from the feldspar components, particularly for blueschist facies mafic rocks. In this case, the feldspars do not project onto the ACF plane with the exception of An and neither does Phe, whereas Gln projects onto the AF binary with a negative A coordinate, like Bt projected from Ms (Fig. 9.5a and b). In metamafic rocks, only one of the K-micas, Phe or Bt, is generally present, which means that the small amount of K_2O present can be ignored. One may also choose to project from Ab (Jd) and Ms. The consequences of the large number of alternatives can be understood by a careful consideration of Fig. 9.5a. Also note that not all possible compositional variations of minerals are shown in Fig. 9.5a (e.g. Jd-Di solid solution). Whatever projection is preferred, it is important to specify the projections on any constructed phase diagrams.

Another complication when dealing with metamafic rocks is the fact that they tend to be much more oxidized than, for example, metapelites. Redox reactions that involve phase components with ferric iron are common and important. Notably, in Grt (Adr-component), Am (e.g. riebeckite- and crossite-components) and Cpx (e.g. Ac-component) a considerable amount of the total iron is usually present as Fe_2O_3 . Also, considerable substitution of Fe_2O_3 for Al_2O_3 occurs in most of the low-grade Ca-Al hydrosilicates such as Prh and Ep. Particularly the presence of Ep always signifies the presence of Fe^{3+} . Magnetite is a widespread oxide phase in metamafic rocks as is ilmenite, and sometimes hematite in very oxidized rocks. A separate treatment of REDOX reactions will not be given in this book but one of the effects of variable $\text{Fe}^{3+}/\text{Fe}^{2+}$ ratios in minerals is a further increase of the variance of the considered assemblages. Consequently, the assemblages can occur over a wider P – T range compared to the situation where all, or most of the iron is present as Fe^{2+} . One may also construct ACF diagrams for a fixed oxygen activity. For instance, the coexistence of Hem and Mag in a rock at a particular P and T will fix a_{O_2} (as discussed in Sect. 3.6.2.4) and the conditions will be rather oxidizing with a significant amount of the total iron of the rock present as Fe^{3+} . The effects on mineral stabilities and compositions can be related, to a large extent, to the $\text{Fe}^{3+}\text{Al}_1$ exchange which forms, for example, Ep from Czo, Mag from Hc and Rbk from Gln. By considering ACF projections as projections parallel to the $\text{Fe}^{3+}\text{Al}_1$

exchange vector, important minerals in metamafic rocks such as Ep, grandite (Ca-Fe³⁺) Grt, Mag and crossite can be represented. Note that Mag does not project to the F apex but to the same projection point as Hc and Mg–Al Spl.

Carbonates are widespread and abundant in low-grade metamafic rocks. Fe-bearing Cal and Ank (Dol) are predominant. Carbonates are also often present in high-grade rocks. Carbonates can be represented on ACF diagrams as explained above. However, any reactions that involve carbonates are in general mixed volatile reactions and must be analyzed accordingly (see Chaps. 3, 6 and 8). The presence of significant CO₂ in an aqueous fluid phase also has effects on pure dehydration reactions that do not involve carbonate minerals (Chap. 3). Compared with pure H₂O fluids, in CO₂-rich fluids hydrates (e.g. Chl, Am) may also breakdown at much lower *T* in rocks that contain carbonates.

Basalts also contain TiO₂ in the wt.% range that usually occurs in one major Ti-phase, i.e. Ttn, Ilm or Rt. If two of these minerals are present, Ti-balanced reactions may be useful for *P–T* estimates, e.g. Ky + 3 Ilm + 2 Qtz = 3 Rt + Grt. Titanium is also present in significant amounts in silicates such as Bt, Am and Grt, with unavoidable consequences for solution properties and equilibrium conditions of reactions.

In conclusion, the composition of metamafic rocks is complex and minerals that typically occur in the assemblages show extensive chemical variation along several exchange directions. This makes comprehensive graphical analysis of phase relationships in metamorphic mafic rocks difficult. The complex chemical variation of solid-solution minerals can be simplified for graphical analysis by projecting parallel to some of the exchange components but the choice of projection depends entirely on the problem one wants to solve and the kind of rocks one is working with. For many metamafic rocks, it turns out that a very advantageous and powerful projection can be made from SiO₂, NaAlO₂, H₂O and CO₂, parallel to MgFe₁ and Fe³⁺Al₁ onto the Al₂O₃–CaO–FeO–mole fraction triangle. This ACF projection will be used below.

The chemical complexity of mafic rocks also makes it difficult to discuss phase relationships by means of chemical subsystems and comprehensive petrogenetic grids and phase diagrams in *P–T* space (as for example such as those used in previous chapters). Note, however, that although the complexity of mafic rocks can be quantitatively analyzed, this must be done individually for each given suite of rocks. The presentation below is thus mainly a discussion of the ACF system and MORB composition with some important reactions discussed separately where necessary.

9.2 Overview of Metamorphism of Mafic Rocks

The best overview of the metamorphism of mafic rocks can be gained from the metamorphic facies scheme shown in Fig. 4.3. As the characteristic assemblages in metabasalts are used for the definition of metamorphic facies they serve as a

reference frame for all other rock compositions and metamafic rock mineral assemblages that are diagnostic for different facies are given in Chap. 4. From Fig. 4.3 it is evident that basalt undergoing prograde metamorphism along a Ky- or Sil-type prograde path will first produce diagnostic assemblages of the subgreenschist facies, followed by greenschist, amphibolite and finally end up as a mafic granulite. High-*P*/low-*T* metamorphism (HPLT metamorphism) transforms basalt into blueschist and then into eclogite. Any geologic process that transports mafic rocks to great depth (>50 km) will result in the formation of eclogite. In contact metamorphism (LPHT metamorphism), basalts are converted to mafic hornfelses. Partial melting of H₂O-saturated metamafics begins at temperatures significantly higher than for metagranitoids, metapsammities and metapelites, e.g. ~850–700 °C between 200–700 MPa, respectively.

Prograde metamorphism of mafic rocks produces sequences of mineral zones that can be compared with mineral zones defined by metapelite minerals such as the example from the low-*P* northern Michigan terrane shown in Fig. 9.6. The metapelites contain Ms and Qtz throughout with And or Sil as the Al-silicates. The corresponding prograde mineral zonation in metabasites shows a series of features that are very characteristic of metamafic rocks.

- There are very few different mineral species present in metamafic rocks. The greenschist facies rocks contain: $\text{Ab} + \text{Chl} + \text{Act} + \text{Ep} \implies$ greenschist. In the amphibolite facies, the minerals are: $\text{Pl} (>\text{An}_{17}) + \text{Hbl} \pm \text{Bt} \pm \text{Ep} \implies$ amphibolite.
- Most minerals occur in many of the mineral zones defined by metapelites.
- The characteristic prograde changes in metabasites relate to the compositions of plagioclase and amphibole.
- Plagioclase systematically changes its composition from Ab at low grade to more calcic plagioclase (andesine). The transition from albite to oligoclase is abrupt and marks a sharp mapable boundary in the field. The discontinuous nature is caused by a miscibility gap in the plagioclase system as shown in Fig. 9.7. This discontinuity can be used to define the greenschist-amphibolite facies boundary, which is clearly transitional and can be designated as a transitional facies (see Fig. 9.7). Along a Ky-type path the oligoclase-in boundary coincides with the staurolite zone boundary that marks the beginning of the amphibolite facies in metapelites. In low-*P* metamorphism (e.g. Fig. 9.6), St occurs for the first time inside the amphibolite facies.
- Amphibole systematically changes its composition from Act at low grade to Na- and Al-bearing Hbl at higher grade (the Hbl color information in Fig. 9.6 relates to the changing mineral composition).
- Quartz is only occasionally present and hence, ACF diagrams must be used with care.
- Biotite is present as an extra K-bearing mineral from the greenschist to upper amphibolite facies and systematically changes its composition during prograde metamorphism, e.g. becomes more Ti and Mg-rich.

Metamorphic facies	Greenschist		Amphibolite		
	Chlorite	Biotite	Garnet	Staurolite	Sillimanite
Mineral zoning					
Metamafites					
Albite	—————			
Albite-oligoclase		—————		
Oligoclase-andesine				—————	
Andesine					—————
Epidote	—————				
Actinolite	—————			
Hornblende		—————		green	green and brown
Chlorite	—————	..			
Calcite			
Biotite		—————		brown	—————
Muscovite
Quartz
Metapelites					
Chlorite	—————			
Muscovite					—————
Biotite		—————			—————
Garnet			—————		—————
Staurolite				—————	—————
Alumosilicate				andalusite	sillimanite
Chloritoid				
Plagioclase	clastic		oligoclase		
Quartz	—————	—————	—————	—————	—————

Fig. 9.6 Progressive mineral changes in metamafic and metapelitic rocks of northern Michigan (after James 1955)

- Calcite is present in low-grade rocks but is used up by mixed volatile reactions during prograde metamorphism.

A comprehensive representation of the effects of metamorphism on mafic rocks is shown in Fig. 9.8. The figure depicts the characteristic assemblages in metabasalts in the form of ACF diagrams representative for the respective position in *P-T* space. The ACF diagrams are arranged along three typical paths of prograde metamorphism and the 9°C km⁻¹ geotherm limits the geologically accessible *P-T* space. The Al-silicate phase relations are given for reference. The inset in the upper left corner shows the composition of typical mid-ocean ridge basalt (Pl + Cpx ± Opx ± Qtz). Many metabasalts are expected to lie compositionally within the horizontally ruled field. ACF diagrams in Fig. 9.8 showing assemblages that represent the approximate composition of MORB have been shaded. Metabasalts that have been strongly metasomatized during ocean-floor metamorphism may project to other compositions in the ACF diagram.

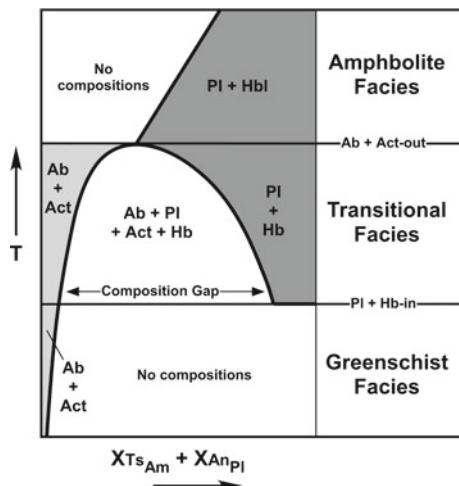


Fig. 9.7 Schematic diagram illustrating the greenschist-amphibolite transition in terms of X_{Ts} (amphibole) and X_{An} (plagioclase) versus temperature at a specified pressure, showing position of a composition gap (=miscibility gap, here peristerite gap in Pl and Ts gap in amphibole) that defines the temperature interval of a transition facies in metabasic (with Am + Pl) and meta-quartzofeldspathic (with Pl) rocks. Pl = oligoclase–andesine compositions. In the greenschist facies albite + actinolite (together with chlorite and epidote) are stable; in the transition facies, the coexisting pairs, albite and oligoclase–andesine, actinolite and hornblende occur; in the amphibolite facies hornblende + oligoclase–andesine are stable

9.2.1 Plagioclase in Mafic Rocks, Equilibria in the Labradorite System (NCASH System)

Figure 9.9 depicts assemblage stabilities in the NCASH system, specifically for the composition of labradorite (1 Ab + 1 An). The composition represents the typical plagioclase of mafic igneous rocks such as basalts and gabbros. This composition and the model of Fig. 9.9 fully describe metamorphism of anorthosite and a large part of the behavior of basalts and gabbros. In the P – T range of Fig. 9.9 plagioclase changes its composition systematically. In the lower right area of Fig. 9.9 Pl is a homogeneous solid solution of labradorite composition. With increasing pressure plagioclase becomes increasingly sodic and the An component of labradorite is transferred to other calcic minerals such as clinozoisite and margarite. In the T -range of the greenschist facies (300–500 °C) and a given Barrovian Ky-type geotherm of 20 °C/km the labradorite composition is represented by the assemblage albite + clinozoisite (epidote) + paragonite + Qtz. As temperature approaches about 520 °C plagioclase drastically increases its An-content and in a small T -interval near 530 °C the stable assemblage is margarite + paragonite + andesine (Fig. 9.9). Above 550 °C labradorite is stable.

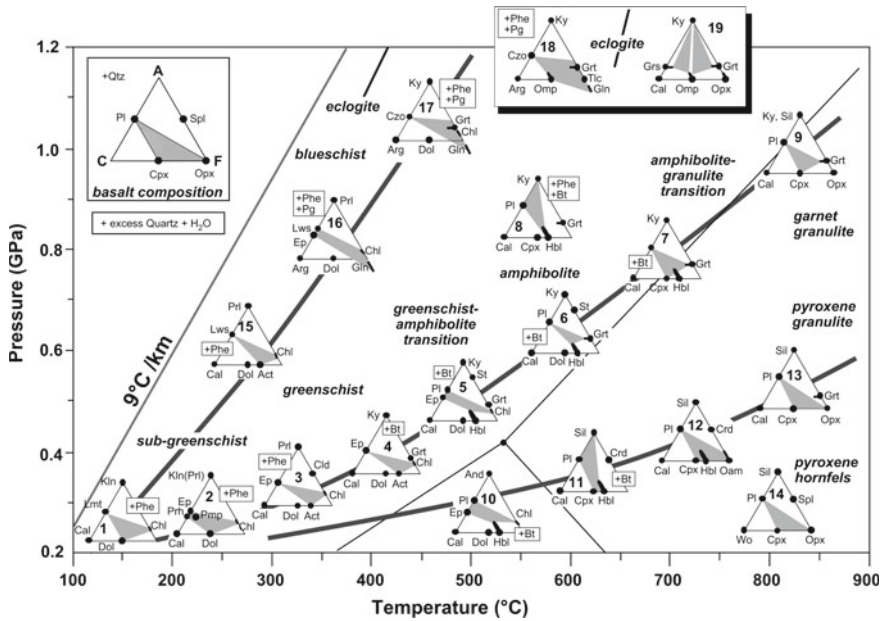


Fig. 9.8 Metamorphism of mafic rocks (metabasalts) represented by ACF diagrams

Along a constant 7 °C/km geotherm for fast subduction, the labradorite bulk composition will be represented by an albite + lawsonite assemblage at temperatures significantly below 300 °C. At $T > 300$ °C jadeite is stable rather than albite (Fig. 9.9). Lws + Jd is the characteristic assemblage in very low- T and high- P metamorphism. At 650 °C and 2.6 GPa the geotherm crosses the boundary to the coesite-stable field.

The considered labradorite-bearing material may detach from the subducting slab at the position indicated by an open diamond on the 7 °C km⁻¹ geotherm (at 2.4 GPa). From there it may follow a characteristic exhumation path along the subduction interface (indicated by a dashed arrow on Fig. 9.9). The typical path is described by an initial stage marked decompression (see Chap. 3). The consequence is that the HPLT assemblage Lws + Jd is replaced by Jd + Czo + Pg at 1.9 GPa (reaction 69 Table 9.2). This dehydration reaction typically runs to completion and replaces all Lws with Czo + Pg. The latter mineral pair forms very commonly pseudomorph textures after Lws, indicating the former presence of the diagnostic HPLT minerals lawsonite in the rocks (Fig. 9.10). Further decompression brings the rock back to the plagioclase present field of Fig. 9.9. The initial Pl so formed at 1.6 GPa along the dashed decompression path is rather pure albite.

Metamorphism along geotherms that reach high- P granulite facies condition produces the characteristic assemblage Czo + Ky and plagioclase becomes more albitic with increasing pressure. Eclogite facies metamorphism creates the same

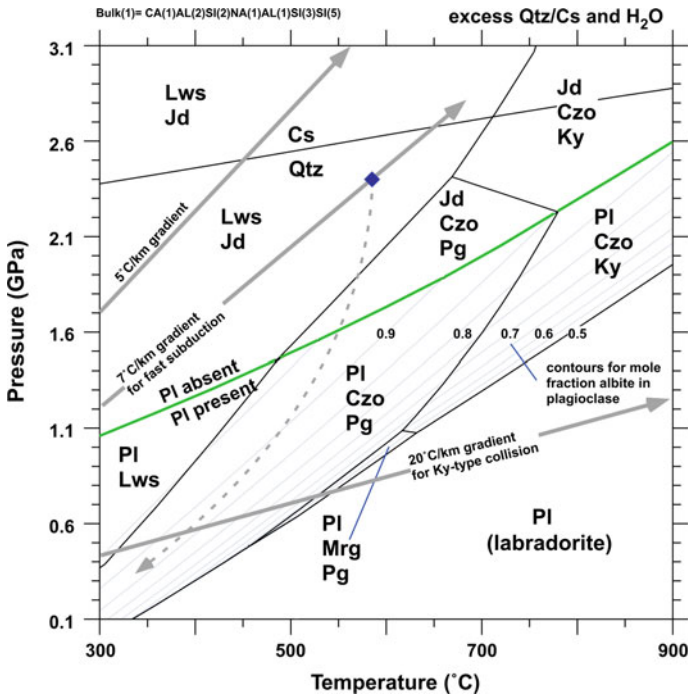


Fig. 9.9 Distribution of stable assemblages for the composition of labradorite and excess Qtz and H_2O . Thin blue lines are mole fraction contours for the Ab-content of plagioclase. Heavy green curve: Plagioclase present—plagioclase absent boundary. Three different geotherms are shown as gray lines. Blue diamond on the fast subduction geotherm is an arbitrary pressure (depth) of detachment from the slab followed by an exhumation path indicated by a dashed gray curve

assemblage Czo + Ky in the PI-absent field of Fig. 9.9. The Czo + Ky is typical of high- T eclogites (see below).

9.3 Subgreenschist Facies Metamorphism

9.3.1 General Aspects

ACF chemographies #1 and #2 (Fig. 9.8) represent mineral assemblages typical of the subgreenschist facies of metamorphism. At very low grade, the characteristic assemblage includes Ab + Chl + carbonate + a variety of zeolites. On the ACF chemography #1, zeolite is typified by Lmt but any of the four zeolites listed in Table 9.1 would project to the same point. In addition, clay (e.g. smectite, Vrm) and “white mica” (Ill, Ser) may be present as well as Kln. At slightly higher grade (ACF chemography #2), zeolites are replaced by Prh, Pmp and Ep in a number of different combinations. Still Ab, Chl and carbonates are major minerals in prehnite-

Table. 9.2 Stoichiometry of reactions in mafic rocks

<i>Subgreenschist facies</i>	
CASH system	
1	$\text{Stb} = \text{Lws} + 5 \text{ Qtz} + 5 \text{ H}_2\text{O}$
2	$\text{Lmt} = \text{Lws} + 2 \text{ Qtz} + 2 \text{ H}_2\text{O}$
3	$\text{Stb} = \text{Lmt} + 3 \text{ Qtz} + 3 \text{ H}_2\text{O}$
4	$\text{Stb} = \text{Hul} + \text{H}_2\text{O}$
5	$\text{Hul} = \text{Lmt} + 3 \text{ Qtz} + 2 \text{ H}_2\text{O}$
6	$\text{Hul} = \text{Wa} + 3 \text{ Qtz} + 4 \text{ H}_2\text{O}$
7	$\text{Lmt} = \text{Wa} + 2 \text{ H}_2\text{O}$
8	$\text{Wa} = \text{Lws} + 2 \text{ Qtz}$
9	$\text{Lws} = \text{An} + 2 \text{ H}_2\text{O}$
10	$\text{Wa} = \text{An} + 2 \text{ Qtz} + 2 \text{ H}_2\text{O}$
11	$\text{Stb} + \text{Grs} = 2 \text{ Prh} + 4 \text{ Qtz} + 5 \text{ H}_2\text{O}$
12	$2 \text{ Prh} = \text{Lws} + \text{Grs} + \text{Qtz}$
13	$5 \text{ Prh} = 2 \text{ Czo} + 2 \text{ Grs} + 3 \text{ Qtz} + 4 \text{ H}_2\text{O}$
14	$5 \text{ Lws} + \text{Grs} = 4 \text{ Czo} + \text{Qtz} + 8 \text{ H}_2\text{O}$
15	$2 \text{ Lws} + \text{Prh} = 2 \text{ Czo} + \text{Qtz} + 4 \text{ H}_2\text{O}$
16	$\text{Prh} + 2 \text{ Lmt} = 2 \text{ Czo} + 5 \text{ Qtz} + 8 \text{ H}_2\text{O}$
17	$\text{Prh} + 2 \text{ Wa} = 2 \text{ Czo} + 5 \text{ Qtz} + 4 \text{ H}_2\text{O}$
NCMASH system	
18	$4 \text{ Hul} + \text{Tr} = 3 \text{ Prh} + \text{Chl} + 24 \text{ Qtz} + 18 \text{ H}_2\text{O}$
19	$4 \text{ Lmt} + \text{Tr} = 3 \text{ Prh} + \text{Chl} + 12 \text{ Qtz} + 10 \text{ H}_2\text{O}$
20	$20 \text{ Pmp} + 3 \text{ Tr} + 6 \text{ Qtz} = 43 \text{ Prh} + 7 \text{ Chl} + 2 \text{ H}_2\text{O}$
21	$86 \text{ Lmt} + 17 \text{ Tr} = 30 \text{ Pmp} + 11 \text{ Chl} + 267 \text{ Qtz} + 212 \text{ H}_2\text{O}$
22	$86 \text{ Lws} + 17 \text{ Tr} = 30 \text{ Pmp} + 11 \text{ Chl} + 95 \text{ Qtz} + 40 \text{ H}_2\text{O}$
23	$5 \text{ Pmp} + 3 \text{ Qtz} = 7 \text{ Prh} + 3 \text{ Czo} + \text{Chl} + 5 \text{ H}_2\text{O}$
24	$6 \text{ Lmt} + 17 \text{ Prh} + 2 \text{ Chl} = 10 \text{ Pmp} + 21 \text{ Qtz} + 14 \text{ H}_2\text{O}$
25	$14 \text{ Lmt} + 5 \text{ Pmp} = 17 \text{ Czo} + \text{Chl} + 32 \text{ Qtz} + 61 \text{ H}_2\text{O}$
26	$86 \text{ Stb} + 17 \text{ Tr} = 30 \text{ Pmp} + 11 \text{ Chl} + 525 \text{ Qtz} + 470 \text{ H}_2\text{O}$
<i>Subgreenschist to greenschist facies transition</i>	
Essential reactions	
27	$5 \text{ Prh} + \text{Chl} + 2 \text{ Qtz} = 4 \text{ Czo} + \text{Tr} + 6 \text{ H}_2\text{O}$
28	$25 \text{ Pmp} + 2 \text{ Chl} + 29 \text{ Qtz} = 7 \text{ Tr} + 43 \text{ Czo} + 67 \text{ H}_2\text{O}$
Additional reactions	
29	$4 \text{ Wa} + \text{Ab} = \text{Pg} + 2 \text{ Czo} + 10 \text{ Qtz} + 6 \text{ H}_2\text{O}$
30	$4 \text{ Lws} + \text{Ab} = \text{Pg} + 2 \text{ Czo} + 2 \text{ Qtz} + 6 \text{ H}_2\text{O}$
31	$14 \text{ Lws} + 5 \text{ Pmp} = 17 \text{ Czo} + \text{Chl} + 4 \text{ Qtz} + 33 \text{ H}_2\text{O}$
32	$4 \text{ Lmt} + \text{Ab} = \text{Pg} + 2 \text{ Czo} + 10 \text{ Qtz} + 14 \text{ H}_2\text{O}$
Reactions involving carbonates (examples)	
33	$3 \text{ Chl} + 10 \text{ Cal} + 21 \text{ Qtz} = 2 \text{ Czo} + 3 \text{ Tr} + 10 \text{ CO}_2 + 8 \text{ H}_2\text{O}$
34	$15 \text{ Pmp} + 9 \text{ Qtz} + 4 \text{ CO}_2 = 4 \text{ Cal} + 25 \text{ Czo} + 3 \text{ Tr} + 37 \text{ H}_2\text{O}$

(continued)

Table. 9.2 (continued)

<i>Subgreenschist facies</i>	
CASH system	
1	Stb = Lws + 5 Qtz + 5 H ₂ O
<i>Greenschist facies</i>	
CMASH reactions	
35	2 Czo + 5 Prl = 4 Mrg + 18 Qtz + 2 H ₂ O
36	Mrg + 2 Qtz + 2 Czo = 5 An + 2 H ₂ O
37	Mrg + Qtz = An + And + H ₂ O
38	4 Mrg + 3 Qtz = 2 Czo + 5 Ky + 3 H ₂ O
39	2 Chl + 2 Czo + 2 Qtz = 2 Tr + 5 Ky + 7 H ₂ O
40	6 Czo + 7 Qtz + Chl = 10 An + Tr + 6 H ₂ O
41	2 An + Chl + 4 Qtz = Tr + 3 Sil + 3 H ₂ O
Example of reaction producing Tschermak (Ts) component	
42	7 Chl + 14 Qtz + 12 Czo = 12 Tr + 25 TS (Al ₁ Al ₁ Si ₋₁ Mg ₋₁) + 22 H ₂ O
Mica-involving reactions	
43	16 Tr + 25 Ms = 25 Phl + 16 Czo + 1 Chl + 77 Qtz + 4 H ₂ O
44	4 Tr + 6 Chl + 25 Cel = 25 Phl + 4 Czo + 63 Qtz + 26 H ₂ O
45	1 Chl + 4 Cel = 3 Phl + 1 Ms + 7 Qtz + 4 H ₂ O
46	2 Chl + 2 Czo + 5 Ab + 4 Qtz = 2 Tr + 5 Pg + 2 H ₂ O
Carbonate-involving reaction (examples)	
47	1 Ms + 3 Qtz + 8 Dol + 4 H ₂ O = 1 Phl + 1 Chl + 8 Cal + 8 CO ₂
48	9 Tr + 2 Cal + 15 Ms = 15 Phl + 10 Czo + 42 Qtz + 2 CO ₂ + 4 H ₂ O
49	19 Cal + 3 Chl + 11 CO ₂ = 15 Dol + 2 Czo + 3 Qtz + 11 H ₂ O
<i>Greenschist-amphibolite facies transition</i>	
50	4 Chl + 18 Czo + 21 Qtz = 5 Ts-amphibole + 26 An + 20 H ₂ O
51	7 Chl + 13 Tr + 12 Czo + 14 Qtz = 25 Ts-amphibole + 22 H ₂ O
52	Ab + Tr = Ed + 4 Qtz
53	12 Czo + 15 Chl + 18 Qtz = 8 Grs + 25 Prp + 66 H ₂ O
<i>Amphibolite facies</i>	
54	4 Tr + 3 An = 3 Prp + 11 Di + 7 Qtz + 4 H ₂ O
55	1 Ts-amphibole + 6 Czo + 3 Qtz = 10 An + 4 Di + 4 H ₂ O
56	3 Ts-amphibole + 7 Ky = 6 An + 4 Prp + 4 Qtz + 3 H ₂ O
57	7 Ts-amphibole + 7 Sil + 4 Qtz = 14 An + 4 Ath + 3 H ₂ O
58	7 Tr = 3 Ath + 14 Di + 4 Qtz + 4 H ₂ O
<i>Amphibolite-granulite facies transition</i>	
59	Tr = 2 Cpx + 3 Opx + Qtz + H ₂ O
60	Ts = Cpx + 3 Opx + An + H ₂ O
61	Tr + 7 Grs = 27 Cpx + Prp + 6 An + H ₂ O
62	Tr + Grs = 4 Cpx + Opx + An + H ₂ O
<i>Granulite facies</i>	
63	4 En + 1 An = 1 Di + 1 Qtz + 1 Prp

(continued)

Table. 9.2 (continued)

<i>Subgreenschist facies</i>	
CASH system	
1	Stb = Lws + 5 Qtz + 5 H ₂ O
<i>Blueschist facies</i>	
64	Tr + 10 Ab + 2 Chl = 2 Lws + 5 Gln
65	6 Tr + 50 Ab + 9 Chl = 25 Gln + 6 Czo + 7 Qtz + 14 H ₂ O
66	13 Ab + 3 Chl + 1 Qtz = 5 Gln + 3 Pg + 4 H ₂ O
67	12 Lws + 1 Gln = 2 Pg + 1 Prp + 6 Czo + 5 Qtz + 20 H ₂ O
68	4 Pg + 9 Chl + 16 Qtz = 2 Gln + 13 Prp + 38 H ₂ O
69	4 Lws + 1 Jd = 2 Czo + 1 Pg + 1 Qtz + 6 H ₂ O
<i>Blueschist-eclogite facies transition</i>	
70	Jd + Qtz = Ab
71	1 Gln + 1 Pg = 1 Prp + 3 Jd + 2 Qtz + 2 H ₂ O
<i>Granulite- and amphibolite-eclogite facies transition</i>	
72	CaTs + Qtz = An
73	2 Czo + Ky + Qtz = 4 An + H ₂ O
74	1 Grs + 2 Ky + 1 Qtz = 3 An
75	4 Tr + 3 An = 3 Prp + 11 Di + 7 Qtz + 4 H ₂ O
76	4 En + 1 An = 1 Prp + 1 Di + 1 Qtz
77	3 Di + 3 An = 1 Prp + 2 Grs + 3 Qtz
78	1 An + 2 Di = 2 En + 1 Grs + 1 Qtz
<i>Eclogite facies</i>	
79	Pg = Jd + Ky + H ₂ O
80	6 Czo + 4 Prp + 7 Qtz = 13 Ky + 12 Di + 3 H ₂ O
81	Tlc + Ky = 2 En + Mg-TS + 2 Qtz + H ₂ O
82	Grs + Prp + 2 Qtz = 3 Di + 2 Ky
83	Grs + 6 Opx = 3 Di + Prp

pumpellyite facies rocks. Pyrophyllite may be present instead of Kln. Zeolite-bearing metamafic rocks indicate temperatures of 150–200 °C or lower, and metabasalts with Prh and Pmp are characteristic for the temperature range 150–300 °C.

Mineral zones mapped in metamafic rocks from the Tanzawa Mountains, central Japan, are shown in Fig. 9.11. The low-*P* Sil-type metamorphic terrain has been subdivided into five zones ranging from lower subgreenschist facies to amphibolite facies. The two lowest-grade zones are characterized by the presence of zeolites, low-*T* zeolites in zone I and high-*T* zeolites in zone II. Zone I zeolites are typically stilbite (Stb) and heulandite (Hul); Zone II zeolites are laumontite (Lmt) and wairakite (Wa). This is understandable by reference to Table 9.1 where it can be seen that zone I zeolites clearly contain more crystal water (zeolite water) than zeolites of zone II. The transition from zone I to zone II is therefore related to dehydration



Fig. 9.10 Clinozoisite (+paragonite) pseudomorphs after lawsonite in retrogressed glaucophanite and eclogite of the Zermatt-Saas meta-ophiolite (Western Alps)

reactions involving zeolites. For the same reason, it is also clear that Wa is typically the highest- T zeolite in prograde metamorphism. Analcite occurs sporadically in both zones and mixed-layer clays are typically present. Plagioclase is present in all zones with the composition of Ab in the zones I–IV. As the mafic protolith is rich in SiO_2 quartz is present as an excess phase throughout (ACF diagrams). No zeolites survive in zone III, which is characterized by three new metamorphic minerals: Prehnite (Prh), pumpellyite (Pmp) and epidote (Ep). Also, Chl has transformed into a well-defined Fe–Mg sheet silicate. Sericite is sporadically present. Several zeolite- and Chl-consuming reactions are responsible for the generation of the new metamorphic minerals Prh, Pmp, and Ep. In zone IV, typical greenschist facies assemblages replace the zone III minerals. In particular, Pmp and Prh disappear and the characteristic greenschist facies mineral association $\text{Chl} + \text{Ep} + \text{Act} + \text{Ab} \pm \text{Qtz}$ becomes dominant. In zone V, close to the igneous contact, the minerals are diagnostic of the amphibolite facies. Calcic plagioclase and Hbl are dominant but Bt, Grt and Cpx may appear as well. In low- P terrains such as the Tanzawa Mountains, cummingtonite or other Fe–Mg amphiboles typically occur together with calcic amphibole (Hbl).

The Tanzawa mineral zones are similar in many ways to that described from recent geothermal systems (<100,000 years old) such as the Nesjavellir geothermal field developed within a sequence of hyaloclastites, basalt flows, dykes and sills of the Hengill central volcano, Iceland. Although the system is now cooling, a highest subsurface T of $>380^\circ\text{C}$ and structures indicate that ascending boiling water from a heat source (probably diorite as at Tanzawa) has mixed with descending cold ground water resulting in the formation of a systematic depth zonation of mineral assemblages ranging from zeolite to amphibolite facies grade in vesicles, veins and

Mineral zoning	zone I	zone II	zone III	zone IV	zone V
Clinoptililite	—————	X	X		
Stilbite	—————	X	X		
Heulandite	—•————				
Mordenite	••••••••				
Chabazite		X	X		
Laumontite		—————	X	X	X
Thompsonite		••••••••			
Wairakite		—————			
Yugawaralite		—————			
Analcime	••••••••	••••••••	••••••••		
Montm.-verm.	—————				
Verm.-chlorite	—————	•••			
Chlorite	—————	•••	—————	—————	•••
Sericite		••••••••	••••••••	••••••••	••••••••
Biotite		••••••••	••••••••	••••••••	••••••••
Pumpellyite		—————	—————	•••	•••
Prehnite		—————	—————	•••	•••
Epidote		•••	—————	—————	•••
Piemontite				••••••••	••••••••
Actinolite				—————	—————
Hornblende				—————	—————
Cummingtonite					••••••••
Diopside					•••
Ca-garnet					•••
Plagioclase				—————	—————
				An ₁₀	An ₂₀ An ₃₀
Opalline silica	••••				
Quartz	—————	—————	—————	—————	—————
Magnetite	—————	—————	—————	••••••••	••••••••
Hematite	••••••••	••••••••	••••••••	••••••••	••••••••
Pyrite	••••••••	••••••••	••••~••••	••••~••••	••••~••••
Calcite	••••~••••	••••~••••	••••~••••	••••~••••	••••~••••

Fig. 9.11 Occurrence of some metamorphic minerals in metamafic rocks, Tanzawa Mountains, central Japan (after Seki et al. 1969). Zone I: Stilbite (clinoptilolite)-vermiculite; Zone II: Laumontite-“mixed layer”-chlorite; Zone III: Pumpellyite-prehnite-chlorite; Zone IV: Actinolite-greenschist; Zone V: Amphibolite. X = only in veins

within the host basalt near zones of high permeability such as brecciated-vesiculated flow tops and fractures (Fig. 9.12). Noteworthy is the sequence of zeolite zonation with Lmt and Wa forming at the highest T of >120 and >200 °C, respectively; the other zeolites forming below about 100 °C. At shallow depths, smectite-type clay minerals occur. With depth they are replaced by interstratified smectite-chlorite at ~ 200 °C, and finally Chl at 230–240 °C. Unlike Tanzawa, Pmp is absent (as in ocean floor metamorphism); Prh appears at >200 °C and Act at >280 °C and Hbl at >350 °C. Albite is the most common feldspar with oligoclase and andesine occurring at deeper levels.

Another well-documented example of prograde zeolite to amphibolite facies thermal metamorphism of metamafic rocks is a >6 km-thick sequence of massive lava flows, pillow lava, breccia and tuff known as the Karmutsen Volcanics at Vancouver Island, British Columbia (Figs. 9.13 and 9.14). Metamorphism occurred at 100–250 MPa and 250–550 °C. The size of inferred equilibrium metamorphic

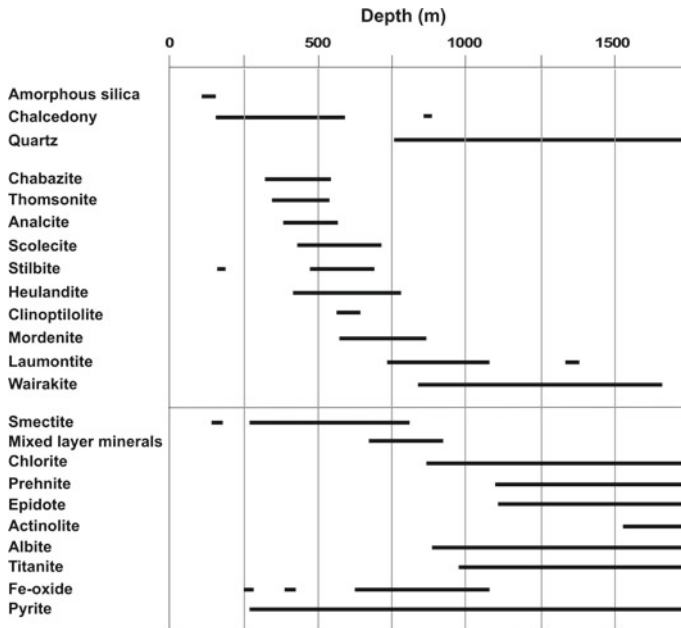


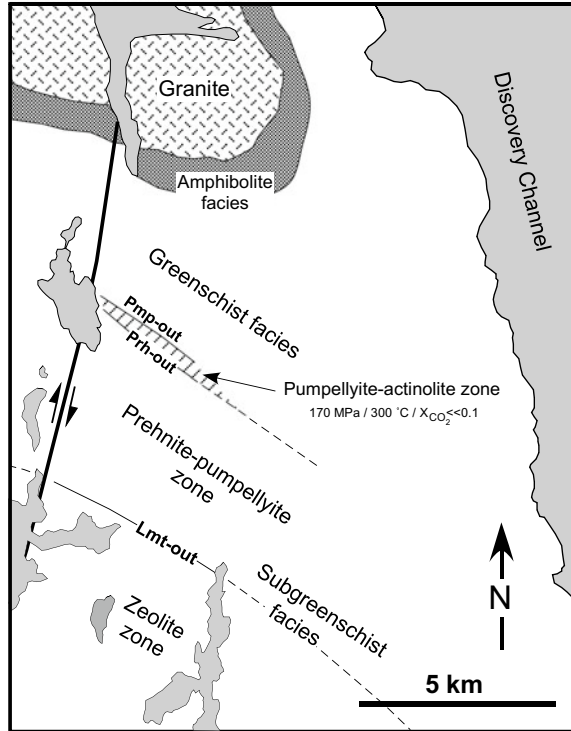
Fig. 9.12 Hydrothermal minerals present at different depths in the Nesjavellir geothermal field, Iceland (well NJ-15) (modified after Fig. 9.13 of Arnórsson 1995)

mineral domains in the rocks is very small and relates to incipient replacement of igneous Cpx, Ca-plagioclase, with more extensive replacement of fine-grained mesostasis and glass. Vesicle (amygdules) assemblages are also considered to represent equilibrium domains and provide the best evidence of prograde metamorphism under subgreenschist facies conditions. The diagnostic calcite-free zeolite facies assemblage is $Lmt + Pmp + Chl + Ep + Ab + Qtz + Ttn \pm Prh$. Prehnite-pumpellyite facies rocks are widespread and contain $Ab + Chl + Pmp + Ttn + Mag \pm Qtz \pm Prh \pm Ep$ with trace $Phe \pm hydro-Grt \pm Wa \pm Cal$, and with vesicles (amygdules) containing $Pmp + Chl \pm Ep \pm Prh \pm Qtz \pm K\text{-white mica} \pm Lmt \pm Wa$. The subgreenschist facies to greenschist facies transition is marked by the appearance of Act without Pmp and a narrow transition zone can be mapped where both Act + Pmp without Prh (and with Ab + Chl + Ep + Cal) define a pumpellyite-actinolite zone (Figs. 9.13 and 9.14).

9.3.2 Metamorphism in the CMASH and NCMASH Systems

Assemblage stabilities in the simple CMASH system in low-grade metamorphism are shown in Fig. 9.15 together with three different geothermal gradients. The stoichiometry of some of the reactions limiting the assemblage fields can be found in Table 9.2. The predicted sequence of Ca-zeolites in progressively

Fig. 9.13 Map showing the zeolite and pumpellyite-actinolite zones of the subgreenschist facies in metamorphosed Karmutsen Volcanics, Vancouver Island, British Columbia (after Fig. 9.1 of Cho and Liou 1987; Fig. 9.1. of Cho et al. 1986 and Fig. 9.1 of Kuniyoshi and Liou 1976)



metamorphosed metamafic rocks along a “very hot” $>30\text{ }^{\circ}\text{C km}^{-1}$ geotherm is: Stb, Hul, Lmt and Wa. This sequence is clearly consistent with the sequence of observed mineral zones in the Tanzawa Mountains shown in Fig. 9.11. This sequence with wairakite as the highest-T zeolite is characteristic for “hot” geothermal environments (geothermal fields, young volcanic areas). Wairakite disappears from the rocks at about $340\text{ }^{\circ}\text{C}$ (Fig. 9.15) and is replaced by the greenschist facies assemblage $\text{Chl} + \text{Act} (\text{Tr}) + \text{Ab} + \text{Qtz}$. In CFMASH rocks Tr is Act and Chl is Fe–Mg chlorite but the assemblages do not shift significantly with Fe as an additional component. Pumpellyite is lacking in hydrothermal hot geothermal sequences (Fig. 9.12). In areas characterized by still “hot” $30\text{ }^{\circ}\text{C km}^{-1}$ gradients the zeolite sequence is: Stb + (Hul) + Lmt but Wairakite does not appear (Fig. 9.15). The zeolite Lmt is replaced by pumpellyite at about $270\text{ }^{\circ}\text{C}$ (black square on dashed $30\text{ }^{\circ}\text{C km}^{-1}$ gradient) defining the zeolite—pumpellyite facies boundary (corresponds to “Lmt-out” mapped on Fig. 9.13). At $315\text{ }^{\circ}\text{C}$ (black circle Fig. 9.15) pumpellyite is replaced upgrade by Czo and Tr that form, together with excess albite, the characteristic assemblage of the greenschist facies (compare with mapped boundary in Fig. 9.13). Along “cooler” gradients, the zeolite facies grades into the pumpellyite facies at lower temperatures. At close to $20\text{ }^{\circ}\text{C km}^{-1}$ the facies transition occurs at about $220\text{ }^{\circ}\text{C}$ and the transition to the greenschist facies is located at T

Facies/Zone	Zeolite	Prehnite-pumpellyite	Pumpellyite-actinolite	Greenschist	Amphibolite
Relic					
Ca-plagioclase				-----	
Augite					..
Fe-oxide					---
Neometamorphic					
Quartz					
Albite					
Plagioclase (>An ₂₀)					
K-feldspar	-----	-----			
Laumontite					
Analcite	---				
Wairakite		---			
Prehnite		-----			
Pumpellyite			-----		
Chlorite					
K-white mica					
Biotite					-----
Actinolite			-----		
Hornblende					-----
Clinopyroxene					-----
Epidote					---
Hydrogarnet		-----	-----	-----	
Titanite					-----
Ilmenite					-----
Magnetite					-----
Hematite					-----
Sulphides					-----
Calcite					-----

Fig. 9.14 Mineral stability ranges with increasing metamorphic grade in basaltic flows, pillows and aquagene tuffs of the Karmutsen Volcanics, Vancouver Island, British Columbia, (see Fig. 9.13)

close to 325 °C. Along “cool” geotherms the pumpellyite facies is lacking. Zeolite assemblages are replaced by lawsonite assemblages. The low-pressure limit of lawsonite assemblages in Fig. 9.15 is near 300 MPa. Along a fast subduction geotherm of 10 °C km⁻¹ stilbite decomposes to lawsonite at *T* as low as 170 °C. The lawsonite assemblages are characteristic for very “cool” low-*T* high-*P* geotherms. They finally grade into blueschist facies and finally eclogite facies assemblages (see below).

Below follows a brief presentation of the typical *P–T* conditions under which some diagnostic index minerals may form and subsequently decompose during prograde metamorphism of metamafic rocks. The discussion is based on Fig. 9.15 with reaction stoichiometries given in Table 9.2.

Analcite (Anl) is commonly found in quartz-bearing diagenetic and low-grade metamorphic rocks. The Anl + Qtz assemblage, along with stilbite (Stb) + Qtz, can be used as an indicator of the initial stage of zeolite facies metamorphism. In the NASH model system, Anl decomposes in the presence of Qtz to Ab according to the reaction: Anl + Qtz = Ab + H₂O (reaction is not listed in Table 9.2). The equilibrium conditions of the Anl breakdown reaction very nearly coincide with the three reactions that limit the Stb field towards higher temperature in Fig. 9.15 [reactions (1), (2), (3) in Table 9.2]. In order to avoid overcrowding, the Anl reaction has not been shown in Fig. 9.15. Natural Anl often shows extensive solid

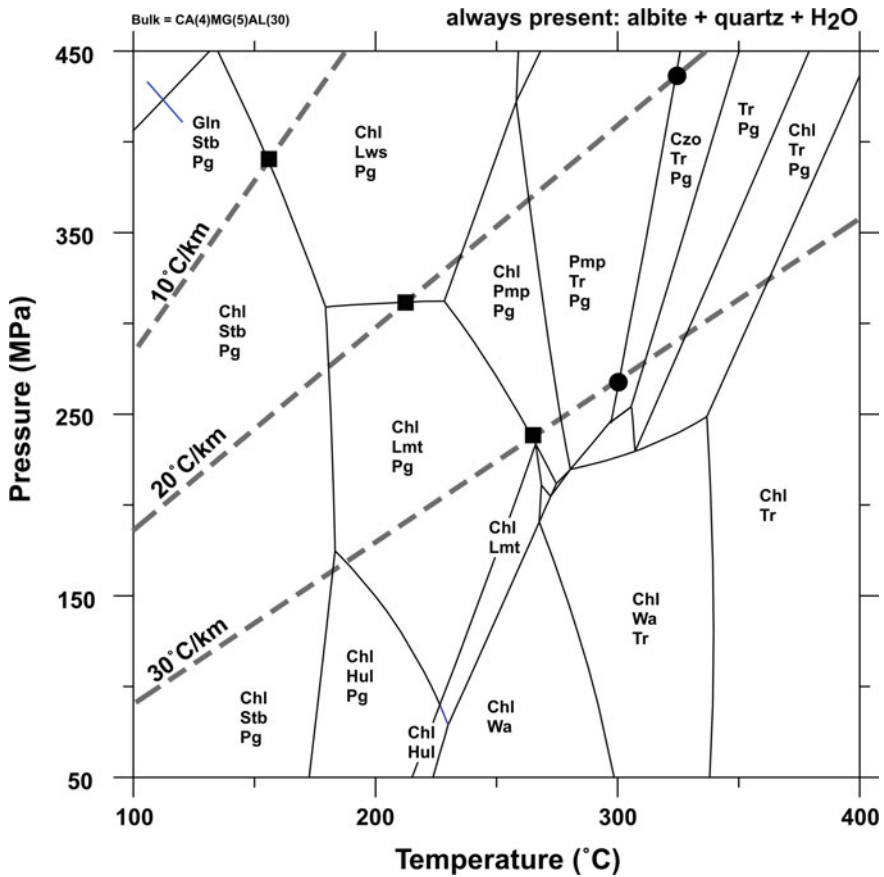


Fig. 9.15 Low-grade metamorphism of metamafic rocks containing Ab and Qtz in excess. Three type-geotherms are shown as dashed lines. Upper *T*-limit of zeolite indicated by black squares, onset of greenschist facies marked by black circles

solution with Wa, thus expanding its stability field to higher *T*. This has the consequence that the *P*–*T* fields of Anl and Hul overlap.

Stilbite, a widespread zeolite mineral, dehydrates to Hul, Lmt or Lws with increasing *T* and successively higher *P* in the CASH model system (Fig. 9.15). However, Stb is occasionally associated with Hul and/or Lmt, e.g. geothermal areas in Iceland (Fig. 9.12). Although little is known about the composition of Stb in low-grade metamorphic rocks, this association may result from solid solution effects. In Alpine fissures Stb may occur together with Lmt and Hul but it always texturally younger than the other zeolites and forms during postorogenic cooling as the latest and “coldest” zeolite.

Heulandite is one of the most common zeolites besides Stb and Lmt. In Fig. 9.15, its stability field is located at temperatures around 200 °C and at pressures

below 200 MPa; and limited by the stability fields of three other zeolites, i.e. Stb towards low- T , Wa towards high- T , and Lmt towards high- P - T . Heulandite and Lmt appear to be equally abundant in ocean-floor thermal, hydrothermal, and burial metamorphism. Laumontite, but not Hul, has been described from subduction zone metamorphism, e.g. from the metabasaltic rocks of the Franciscan terrane, California, and the Sanbagawa Belt, Japan (see Liou et al. 1987 for a summary). This may indicate that Hul is a low- P zeolite consistent with the topology shown in Fig. 9.15.

Natural Hul commonly contains Na or K or both substituting for Ca, and its chemical composition may extend to those of clinoptilolite and alkali-clinoptilolite. This effect, together with other variables (e.g. pore-fluid chemistry), may explain the considerable overlap between the stability regions of Hul and other zeolites (see Figs. 9.11 and 9.12).

Laumontite is widespread in ocean-floor, burial, and subduction zone metamorphism. The field of stable Lmt occurrence in Fig. 9.15 is limited by five univariant reactions. With increasing T , Lmt is formed from Hul at lower P and from Stb at higher P . The upper P limit of Lmt with respect to Lws is about 300 MPa, and the upper T limit with respect to Wa and Ep (Czo) is about 230–260 °C. Lmt is usually near its ideal composition, $\text{CaAl}_2\text{Si}_4\text{O}_{12} \cdot 4\text{H}_2\text{O}$, but solid solution in Hul and Wa will allow the coexistence of Lmt + Hul and Lmt + Wa.

The presence of Lmt is often taken to indicate low-grade metamorphic conditions, and thus its lower thermal stability limit is of interest. In the CASH model system, this limit is about 180 °C. From field evidence, however, it has been inferred that Lmt could have formed at temperatures as low as 50 to 100 °C (e.g. Boles and Coombs 1975).

In Alpine fissures Lmt is very common, although rarely observed in surface outcrops because of its susceptibility to fast decay if exposed to the atmosphere. However, laumontite is the absolutely dominant zeolite in basement rocks found during tunnel constructions in the Alps where the fissure minerals have not been in contact with the atmosphere (Weisenberger and Bucher 2010).

Wairakite is restricted to areas with high thermal gradients, including geothermal systems and areas with intrusive igneous bodies. In the CMASH model system, Wa is produced from Hul or Lmt at temperatures between 220–260 °C. As stated above, Wa has the highest thermal stability of any zeolite (Fig. 9.15) and, in the presence of excess Ab + Qtz, its upper thermal stability is at 340 °C. Wairakite also shows considerable solid solution with Anl that may explain the natural occurrence of Wa + Anl and Wa + Lmt (+ Ab + Qtz). It is remarkably absent from alpine-type orogenic belts.

Lawsonite is one of the most definitive of blueschist facies minerals.

Pumpellyite is a very common mineral in metamafic rocks. It is found in various associations in low-grade rocks (Fig. 9.1a and text). Pmp stability in Fig. 9.15 ranges from 220 to 320 °C at $P > 300$ MPa. Reactions forming and consuming Pmp are listed in Table 9.2. In rocks that depart from the average meta-MORB, Pmp may occur over a much larger or much smaller P - T interval. However, for all rock compositions the center of the Pmp stability fields clusters around 270 °C \pm 20°

and 400 ± 200 MPa. Most Pmp-bearing rocks probably formed close to 250°C and at pressures of 100–300 MPa.

Prehnite occurs widespread in low-grade metamafic rocks as a part of the matrix assemblage but also very often in vesicles, veins and open fractures. Prh fields do not appear for the chosen bulk in Fig. 9.15. The assemblage prehnite + pumpellyite has been used to define a separate Prh—Pmp facies between the zeolite and the greenschist facies. However, it is evident from Fig. 9.15 and also from field occurrences that Prh rarely occurs in stable equilibrium with Pmp and thus the 2-phase assemblage is not well suited to define a metamorphic facies. It is in contrast evident from Fig. 9.15 that Pmp-involving assemblages may occur characteristically in the T -range between zeolite-bearing rocks and greenschist facies rocks. Pmp assemblages may, however, be absent at very high- and very low- T geotherms (Fig. 9.15).

9.3.3 Transition to Greenschist Facies

The transition to the greenschist facies is marked by the first appearance of the diagnostic assemblage Act + Ep in the presence of Chl, Ab and Qtz. The assemblage is produced from Wa decomposition at low- P (<200 MPa) and Pmp decomposition at higher P (>200 MPa). Both reactions [reactions 9.27 and 9.28] produce the typical greenschist facies mineral assemblage at about $320^\circ\text{C} \pm 30^\circ\text{C}$. Along the characteristic prograde metamorphic paths (20 and 30°C km^{-1}), the occurrence of Act + Ep + Chl + Ab + Qtz without Pmp defines the beginning of the greenschist facies. The greenschist facies assemblage is shown on chemography #3 in Fig. 9.8. Chemography #3 also suggests that the greenschist facies assemblage may also form from Dol- or Cal-involving reactions [an example is reaction 9.33]. As carbonates are present in many low-grade mafic rocks, these mixed volatile reactions are important in removing carbonate minerals at an early stage of prograde metamorphism in connection with the formation of greenschist facies minerals. Typically, these reactions consume Chl and carbonate and produce Act + Ep and are maximum-type mixed volatile reactions (see Chaps. 3 and 6). Note, however, that Pmp- and Prh-consuming reactions may *produce* rather than consume carbonates. Reaction 9.34 is an example that limits Pmp formation in the presence of CO_2 -bearing fluids and produces the greenschist facies assemblage. Accordingly, if fluids contain CO_2 , greenschist facies assemblages may appear at lower T compared to pure H_2O fluids.

At high P (e.g., along a low- T 10°C km^{-1} subduction geotherm), subgreenschist facies assemblages are replaced by assemblages diagnostic of blueschist facies conditions. These rocks contain Gln, Lws, Pg, Ep, and other minerals in various assemblages and will be discussed below.

9.4 Greenschist Facies Metamorphism

9.4.1 Introduction

Greenschist facies mafic rocks are, as the name suggests, green schists. The green color of greenschist results from the modal dominance of green minerals in the rocks notably Chl, Act, Ep and these minerals together with $Ab \pm Qtz$ are the most characteristic assemblage of greenschist as stated above. The term *greenschist* is exclusively reserved for schistose chlorite-rich rocks derived from mafic igneous rocks that were metamorphosed under greenschist facies conditions. Note, however, that Pmp + Ep + Chl schist or semi-schist of the subgreenschist facies are also green schists, though obviously not of greenschist facies grade. Schistose serpentinites may also be green schists of the greenschist facies, but they are not classified as greenschist because they are derived from ultramafic rocks such as peridotite.

Chemographies #3 and #4 (Fig. 9.8) represent the typical range of assemblages in the greenschist facies. In addition to the most important minerals named above, other phases such as Ms (Phe), Bt, Stp, Ttn, Cal, Mag or Hem can often be present in minor amounts. Greenschists have also commonly lost all relic structures from previous metamorphic and magmatic stages so that they are both mineralogically and structurally equilibrated.

9.4.2 Mineralogical Changes Within the Greenschist Facies

The difference between chemography #3 and #4 (Fig. 9.8) is the presence of Prl and Phe in the lower greenschist facies and of Ky and Bt in the upper greenschist facies. Phase relationships in the ASH system that covers changes at the A apex of ACF diagrams have been discussed in Chap. 7 and are shown in Fig. 7.3.

Inside the Chl-Ep-Act triangle of Fig. 9.8, there are also reactions that modify the typical greenschist facies assemblage. The processes are best explained by using reaction 9.42 as an example. This reaction describes the production of the TS-component in Am and Chl and the Al-contents of both minerals change systematically (become more Al-rich) with increasing grade across the greenschist facies. The effect can be shown on ACF diagrams by a displacement of the Chl + Ep + Act triangle along the TS vector, but note that concurrent rotations of FM relationships cannot be displayed. AF relationships are complex and can be evaluated along the lines described in Chap. 7. Furthermore, REDOX reactions may change the composition of Ep and other Fe-bearing minerals.

9.4.2.1 Reactions Involving Micas

Muscovite (K-white mica, sericite, phengite) is the most common K-bearing mineral in low-grade metamafic rocks and this is also true for the lower greenschist facies. However, in the middle of the greenschist facies (~400 °C), Bt appears for the first time in metamafic rocks replacing K-white mica. This is shown in Fig. 9.8

(chemographies #3 and #4). Biotite formation relates to reaction 9.43, which involves all greenschist minerals and transfers Ms component to Phl component. The equilibrium of reaction 9.43 is close to 600 °C in the pure KCMASH system and it is rather pressure insensitive. For real mineral compositions of greenschist facies rocks, the formation of Bt from reaction 9.43 takes place around 400 °C. The color of the first Bt that appears during prograde metamorphism of mafic rocks is often green. This is an indication of high Fe^{3+} and demonstrates the importance of REDOX reactions in low-grade metamafic rocks (one must bear this in mind when calculating phase relationships involving Bt).

The production of Bt is a continuous process. The Bt-producing reaction 9.44 is similar to reaction 9.43 except that it consumes the celadonite (Cel) component of K-white mica in order to produce Bt and leaves behind a white mica that is closer to the Ms end-member composition. This is in accordance with field evidence that K-white mica becomes progressively depleted in the Cel-component and enriched in Ms-component along a Ky-type path of prograde metamorphism. The effect can also be understood by investigating reaction 9.45, where the Cel-component is consumed in white mica and Bt + Ms components are formed with prograde metamorphism.

Again, Bt forms in metamafic rocks at about 400–450 °C. K-white mica is typically celadonitic (Phe, Ser) in low-grade rocks and becomes more muscovitic (Ms) towards the upper boundary of the greenschist facies. The small amount of K_2O in mafic rocks is usually bound in K-white mica below 400 °C and in Bt at temperatures above 400 °C, and there is little overlap of the two micas.

Paragonite occurs in greenschists at high-*P*. The equilibrium conditions of reaction 9.46 are extremely sensitive to small compositional variations in the protolith and the resulting metamorphic minerals. However, the typical Act + Pg assemblage forms, at pressures above about 600 MPa, and at this *P* its stability is insensitive to *T*.

9.4.2.2 Garnet, Stilpnomelane and Carbonate

Garnet may form in mafic schist from reactions very similar to those that form Grt in pelitic schist. The first Grt to form is manganiferous and contains only a small Grs-component. Garnet first appears in the higher-grade part of the greenschist facies at relatively high-*P*, but Grt (typically less Mn-rich) is not common in mafic rocks until amphibolite facies conditions are attained.

Stilpnomelane is a characteristic mineral in many low-grade mafic schists and, if present, is diagnostic of lower greenschist facies conditions (or blueschist facies). The brown color of this pleochroic mineral (the oxidized ferristilpnomelane variety) often resembles Bt under the microscope and can easily be mistaken for such. Stilpnomelane is replaced by green Bt at around 400 °C and mafic rocks containing both Stp and Bt may occur over a narrow temperature interval near this temperature.

Carbonate minerals such as Dol (Ank) and Cal are commonly present in greenschists and participate in many mixed volatile reactions that involve the characteristic greenschist facies silicates, Act, Chl and Ep. The reactions may also involve micas such as reaction 9.47 that replaces K-white mica by Bt in Dol- and

Cal-bearing metamafic rocks. Another example is reaction 9.48 where the assemblage Act + Ms + Cal is replaced by Ep + Bt. Reaction 9.49 involves two carbonates in rocks containing Ep + Act. Some of the carbonate-involving reactions are also relevant for marbles (CMS-HC system) or for marly rocks and these have been discussed in Chaps. 6 and 8. There is, however, a great potential for obtaining useful information regarding fluid compositions from carbonate-bearing greenschists.

9.4.3 Greenschist-Amphibolite Facies Transition

The greenschist facies assemblage experiences two basic mineral changes between 450–550 °C:

- Ab disappears and is replaced by oligoclase (typically An₁₇₋₂₀).
- Act takes up increasing amounts of Al and Na and is eventually replaced by Na-bearing aluminous Hbl.

The combined transformation results in the replacement of the Ab + Act pair by the Pl + Hbl pair. This transformation designates the transition from greenschist facies to amphibolite facies conditions. In orogenic metamorphism along a Ky-type prograde path, the greenschist-amphibolite facies transition occurs at temperatures at 500 ± 50 °C (400–500 MPa).

The An-component in Pl is produced by a series of continuous reactions. However, greenschist Ab does not continuously change its composition along the albite-anorthite binary. At upper greenschist facies conditions, the Pl solid-solution series is not continuous but rather shows at least three miscibility gaps. The peristerite gap between Ab (up to An₁₀) and oligoclase (An₁₇) is the most important of these gaps (Fig. 9.7). Because of the abrupt appearance of oligoclase due to the miscibility gap, the first appearance of plagioclase of An₁₇ can be used to define an *oligoclase-in isograd* in mafic as well as pelitic and psammitic schist and denotes the *lower grade limit* of the greenschist—amphibolite facies transition zone. With increasing grade, Ab and oligoclase coexist, with Ab becoming more Ca-rich and oligoclase becoming more Ab-rich defining the miscibility gap until it closes with the disappearance of Ab. The disappearance of Ab also represents an isograd, the *Ab-out isograd* that marks the *upper grade limit* of the transition zone and the beginning of amphibolite facies conditions where oligoclase is the only plagioclase. Unfortunately, the oligoclase-in and albite-out isograds can only be determined by microscope examination. With high-*T* gradients of contact metamorphism, the transition from greenschist to amphibolite facies can be abrupt with only a narrow or no transition zone containing coexisting albite and oligoclase, such as in the Karmutsen Volcanics (Figs. 9.13 and 9.14). In this case, an abrupt change from Ab (An₀₋₄) to oligoclase (An₂₀) occurs that reflects the peristerite composition gap. The

systematic compositional changes in the amphibole solid-solution series are generally more continuous in nature (although an Act—Hbl miscibility gap also exists). Throughout the T - P range of the transition zone Act composition changes by: (1) taking up Ts-component produced by a series of continuous reactions, (2) incorporation of edenite (Ed)-component produced by Ab-consuming reactions, and, (3) the inevitable FM-exchange. Other effects are related to incorporation of Ti and REDOX reactions. The resulting single amphibole is a dark-green tschermakitic to pargasitic hornblende that together with Pl constitutes, by definition, an amphibolite and defines the beginning of the amphibolite facies. Chemography #5 (Fig. 9.8) shows this new situation; Am has changed its composition along the TS-exchange direction and Pl appears on the ACF projections. The most important mineralogical changes within the greenschist-amphibolite transition can be related to three main reactions (Table 9.2). Reaction 9.50 consumes greenschist Ep and Chl and produces the An-component of Pl and Ts- component of Am. Although the reaction will eventually consume all Ep or all Chl, Chl-, and/or Ep-bearing amphibolites may be present in the lowest grade amphibolite facies. All three main minerals of the greenschist facies assemblage (Act, Chl, Ep) are consumed by reaction 9.51 to produce Ts- component in Am, and reaction 9.52 describes the formation of the Ed-component in amphibolite facies Hbl. Thus, the combined effect of the three reactions results in the gradual disappearance of Chl + Ep, increasing Ca-enrichment of Pl, and a systematic change in Am composition from Act to Hbl.

Garnet may also appear in metamafic rocks transitional to the amphibolite facies. Its formation, as in metapelitic and psammitic rocks, mainly occurs at the expense of Chl. Reaction 9.53 indicates that Chl contributes the Prp- (and Alm-) components and Ep produces the Grs- (and Adr) components in Grt. The Mn (Sps)-component (abundant in early-formed Grt) is also supplied by the breakdown of Chl or in some cases, from Ank decomposition. In metamafic rocks, Grt may appear at temperatures of 400–450 °C depending on P .

9.5 Amphibolite Facies Metamorphism

9.5.1 Introduction

The amphibolite facies is characterized by chemography #6, #7 and #8 (Fig. 9.8) and Pl and Hbl make up the bulk volume of amphibolitic metamafic rocks, amphibolites. Much smaller amounts of other silicate minerals include Qtz, Ep, Ms, Bt, Ttn, Grt, and Cpx. Calcite can be found in some amphibolites. Mineralogical changes within the amphibolite facies mostly result from continuous reactions that operate over a wide P - T range. The main effect of these continuous reactions produces systematic variations in the compositions of Pl and Hbl, and decreasing amounts of Ep-Czo and Ms if they persist beyond greenschist facies conditions. Garnet becomes modally more important with increasing grade to form garnet-amphibolite and Cpx appears at higher temperatures in the amphibolite facies.

In principle, given a rock of MORB composition and the compositions of Pl and Hbl, the P – T conditions of equilibration are uniquely defined. However, at present, experimental data do not permit a rigorous treatment of Pl–Hbl relationships. In particular, solution properties of amphiboles are still poorly known and few end-member phase components are well constrained. Surprisingly, the low- T behavior of the plagioclase system is also not quantitatively known (e.g. quantitative thermodynamic description of the several miscibility gaps and structural transitions along the Ab–An binary at low T). This remains true also for the 2022 edition of this book.

9.5.2 Mineral Adjustments Within the Amphibolite Facies

In prograde orogenic metamorphism of metabasalts, the rocks contain Hbl and Pl (oligoclase) at the beginning of the amphibolite facies (~500 °C) as explained in Sect. 9.4.3. In addition, amphibolites may still contain some Ep and/or Chl that has not been completely consumed by reactions that produced the An- and Ts-components in Pl and Hbl, respectively. Biotite may be present as well. The same continuous reactions that produced the amphibolite facies mineralogy initially continue to consume Chl and Ep within the lower grade part of the amphibolite facies until Chl eventually disappears at about 550 °C and Ep is not typically found in amphibolites that were metamorphosed to ~600 °C. Some of the Ep- and Chl-consuming reactions produce Grt that, in general, becomes modally more important with increasing grade. Chemography #6 in Fig. 9.8 is characteristic for the mid-amphibolite facies at ~600 °C. Here, amphibolites typically contain andesine and green Hbl \pm Grt \pm Bt. At still higher temperatures, chemography #7 indicates the appearance of Cpx of the Di–Hd series at ~650 °C (along a prograde Ky-path) [reaction 9.54]. The reaction simultaneously produces Cpx and Grt, and is typical of relatively high- P . However, Cpx is also often found in amphibolites lacking Grt and a typical assemblage is Hbl + Pl + Cpx + Bt. Reaction 9.55 produces Di- and An-components from Am and Ep or Zo. This important reaction has several significant effects: (1) it continuously consumes Ep or Czo that may still be present in mid-amphibolite facies rocks and eventually eliminates them, (2) the reaction consumes amphibole, a process typical in the higher amphibolite facies, (3) the reaction produces Cpx that appears in higher-grade amphibolites, (4) the reaction produces more An- component that is incorporated in plagioclase in high-grade amphibolites. Plagioclase in high-grade amphibolites thus becomes progressively more calcic and in the upper amphibolite facies, andesine-labradorite compositions (An_{30–70}) are typical, although bytownite or anorthite compositions have also been reported.

The first appearance of Cpx in amphibolites can be used to define the lower grade boundary of the upper amphibolite facies. Reactions in the upper amphibolite facies, such as 9.54 and 9.55, begin to break down Am components and replace them with pyroxene components. This is a continuous process, and the first appearance of Cpx in mafic rocks is not usually a sharp isograd in the field. Nevertheless, the “Cpx-in” transition zone marks the beginning of the upper

amphibolite facies and indicates a representative temperature of about 650 °C. Under upper amphibolite facies conditions in water-saturated environments, metamafic rocks show the first structural evidence in the field of local partial melt formation, migmatization and appearance of quartzofeldspathic seams, patches, veins (leucosomes) and similar mobilisate structures. The migmatization processes removes Qtz, Pl, Hbl (and Bt if present) from the rocks and transfers their oxide components to a granitic (trondjemite, tonalite, granodiorite, =TTG) melt phase (leucosome) and a granulite Grt ± Cpx restite. In a generalized form, migmatization of metabasalts (oceanic crust) produces igneous rocks that are typical constituents of continental crust (TTG).

At higher P than that of the ordinary Ky-geotherm (Fig. 9.8), mafic amphibolites may contain the diagnostic Ky + Hbl assemblage Hbl which may have formed by reaction 9.39 earlier in the course of prograde metamorphism. The link to the more common Pl + Grt assemblage found in amphibolites is given by reaction 9.56. This reaction replaces the Grt + Pl tie-line of chemographies #6 and #7 by the Ky + Hbl tie-line of chemography #8. The continuous dehydration reaction runs typically between chemography #6 and chemography #8 in Fig. 9.8 for typical metabasaltic compositions. Therefore, Ky-bearing amphibolites are diagnostic of high- P amphibolite facies (typically greater than 700 MPa). It should be remembered, however, that a Ky + Hbl + Grt + Pl assemblage is not normally co-planar (as one may erroneously conclude from ACF diagrams in Fig. 9.8) but rather defines a phase volume that occurs over a relatively wide P - T interval.

9.5.3 Low-Pressure Series Amphibolites

At low metamorphic grades, mafic rocks metamorphosed along a prograde Ky-type or Sil-type path have very similar mineral assemblages. The most significant difference is the composition of Chl and, especially, K-white mica. The Cel- component of K-white mica is relatively sensitive to variations in P and is controlled by reactions such as 9.45. The Ts-component in mica (and in principle also Chl or Bt) can be used to monitor P conditions in low-grade metamorphism.

The transition to amphibolite facies at low- P is similar to the one described in Sect. 9.4.3. In Al-rich rocks, And may appear instead of Ky (chemography #10 in Fig. 9.8). However, examples of And + Am are rare. Because the reactions that produce amphibolite from greenschist are ordinary continuous dehydration reactions, the transition to the amphibolite facies occurs at slightly lower T for low- P metamorphism. The lower boundary of the amphibolite facies along a Sil-path is typically at about 450 °C (at 300 MPa). Reactions 9.36, 9.37, 9.40 and the And-equivalent of reaction 9.41 pass through the And field in Fig. 9.8. The reactions generally produce An and Hbl components from greenschist facies mineralogy. At 550 °C Ep and Chl typically disappear from low- P amphibolites and the characteristic assemblage is Hbl + Pl ± And ± Bt.

Compared with orogenic metamorphism along a prograde Ky-path, Cpx forms at significantly lower T in low- P amphibolites (600 °C or lower). Chemography #11 in

Fig. 9.8 is characteristic of amphibolites that formed in the range of 300–400 MPa. It shows the usual Hbl + Pl assemblage together with Cpx and Bt. Sillimanite may be present in Al-rich amphibolites and the Sil + Hbl pair forms a stable, though rare, assemblage. However, Grt is scarce or even absent in low-*P* amphibolites.

Chemography #12 in Fig. 9.8 is representative for amphibolites of upper amphibolite facies grade at low-*P* (Sil-path). The most significant feature is the presence of Fe–Mg amphiboles such as anthophyllite (Ath), cummingtonite (Cum), gedrite (Ged) in addition to the Cam (Hbl). In some amphibolites even three different amphibole species may be present such as, e.g. Hbl, Ged and Ath. The abbreviation “Oam” for orthoamphibole in Fig. 9.8 includes all Fe–Mg amphiboles and Ged. Phase relationships in such multi-amphibole rocks can be very complex and miscibility gaps in various amphibole series as well as structural changes in amphiboles are additional complications. However, such low-*P* amphibolites possess a great potential for detailed analysis of relationships among minerals and assemblages and for the reconstruction of the reaction history of low-*P* amphibolites. Fe–Mg-amphiboles may form by a number of different conceivable mechanisms. The first and obvious one is reaction 9.57 that links chemographies #11 and #12. The reaction breaks down a Hbl + Sil assemblage producing An component in Pl. It also produces Ath component in Fe–Mg-amphibole. As metamorphic grade increases, reaction 9.58 becomes more important in producing the Ath-component. The reaction consumes Cam and replaces it with Cpx and Oam. The equilibrium of reaction 9.58 in metamafic rocks involves phase components of the typical assemblage: Hbl + Oam + Cpx + Pl \pm Qtz. As a general rule of thumb, this assemblage is characteristic for temperatures of 650–750 °C along a prograde Sil-type geotherm.

An example of Sil-type amphibolite facies metamorphism is the area of central Massachusetts, USA, where Qtz- and Pl-bearing upper amphibolite facies mafic rocks contain assemblages with a number of coexisting amphiboles; Hbl, Hbl + Cum, Hbl + Oam, Hbl + Oam + Cum (Oam includes Ged and Ath) depending on rock Mg/(Mg + Fe) ratios. In addition to forming single, homogeneous crystals, Hbl contains exsolution lamellae of Cum, Cum contains exsolution lamellae of Hbl, and Ged has exsolved Ath. Metamorphism is estimated to have occurred over an interval of about 580–660 °C, and at higher *T* the amphibolite assemblages were transformed into two pyroxene (Opx + Cpx) \pm Grt granulites (Hollocher 1991).

9.5.4 Amphibolite-Granulite Facies Transition

Much of the Qtz that has been produced during subgreenschist facies to greenschist facies metamorphism is consumed by continuous reactions in the amphibolite facies so that many amphibolites are quartz-free (use ACF diagrams with care!). Most of the water bound in hydrous minerals has also been released by dehydration reactions during prograde metamorphism and metamafic rocks that have been progressively metamorphosed to 700 °C, contain Pl + Hbl \pm Cpx \pm Grt \pm Bt (Ky-path) and Pl + Hbl \pm Cpx \pm Oam \pm Bt (Sil-path). Amphibole is the last

remaining hydrous phase and further addition of heat to the rock by tectono-thermal processes will ultimately remove it. The transition from a relatively hydrous amphibolite facies assemblage to a completely anhydrous granulite facies assemblage is gradual and takes place over a temperature interval of at least 200 °C (from about 650–850 °C). The first clear and unequivocal indication that granulite facies conditions have been attained is the appearance of Opx in Cpx-bearing Qtz-free rocks. Granulite facies conditions are obvious if Opx occurs in Qtz-bearing amphibolites. Orthopyroxene is most common in low-*P* mafic granulites, whereas at higher *P* the typical anhydrous granulite facies assemblage is Pl + Cpx + Grt ± Qtz. The reactions that eventually produce this assemblage are continuous in nature and the *T*-interval is very wide. Hornblende gradually decreases in modal amount, leaving behind an anhydrous granulite facies assemblage. Note, however, that Pl + Cpx + Grt may also occur in the amphibolite facies and that such an assemblage is not necessarily diagnostic of granulite facies conditions. If pressures are too high for Opx to form, then the ultimate granulite facies conditions are reached when Am has disappeared from the rock. Reactions 9.59 to 9.62 in Table 9.2 consume the major Am- components Tr and Ts and produce pyroxene-, Grt- and Pl- components and, hence, represent the transition of amphibolite to granulite facies (Fig. 9.16). In particular, reaction 9.60 is important as it decomposes Hbl to form the two-pyroxene (Cpx + Opx) assemblage diagnostic of the granulite facies in Qtz-absent mafic rocks. In addition, the reaction produces An-component that leads to the presence of Ca-rich plagioclase (labradorite) in mafic granulites.

What happens to Bt during the amphibolite to granulite facies transition? Biotite is a subordinate (accessory) hydrous phase in high-grade amphibolites. The small amount of K₂O typically present in amphibolitic metamafic rocks is mostly stored in Bt and will either be taken up by pyroxene and ternary feldspar or becomes incorporated into a Kfs-Ab-Qtz melt during migmatization. However, as the total amount of water that can be stored in high-grade amphibolites is also very small (on the order of 0.4 wt.% H₂O or less), mafic rocks are less susceptible to partial melting compared to their metapelitic, metapsammitic or metagranitoid counterparts.

9.6 Granulite Facies and Mafic Granulites

The chemographies #9 and #13 in Fig. 9.8 represent granulite facies metamorphism of mafic rocks. At high-*P* the characteristic assemblage is: Pl + Cpx (augite) + Grt. At lower *P* the typical granulite facies assemblage is: Pl + Cpx (augite) + Opx (hypersthene). The two assemblages are linked by the important reaction 9.63 which separates a field of two pyroxene granulites at *P* below about 500–700 MPa from a field of garnet granulites limited by the eclogite field towards high-*P*. The continuous nature of reaction 9.63 generates a wide overlap zone where both Grt and Opx are present in Pl + Cpx rocks. If restricted to meta-MORB compositions,

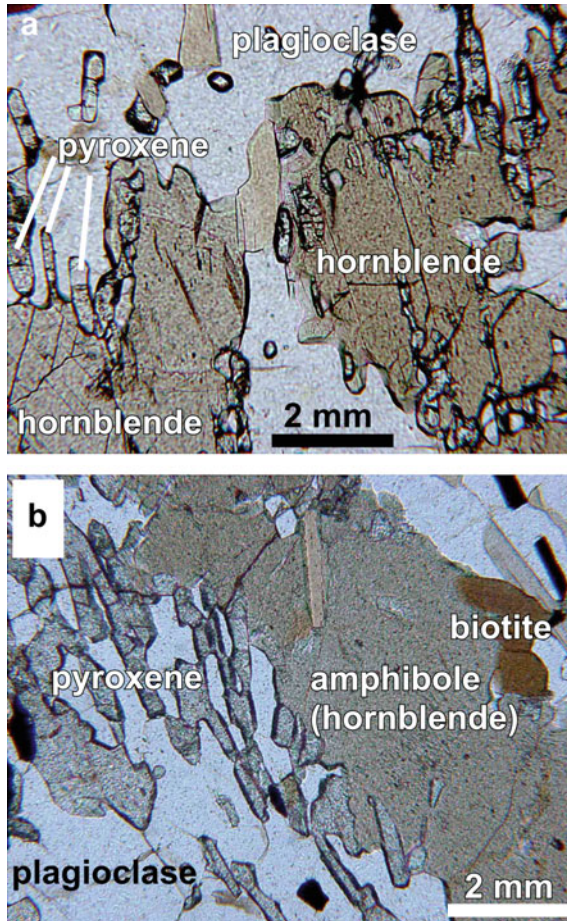


Fig. 9.16 Photomicrographs of mafic rocks from the Thor Range (E-Antarctic shield; Bucher and Frost 2006) showing structures that indicate the prograde breakdown of hornblende to pyroxene and plagioclase (reactions 9.59 and 9.60 Table 9.2). The texture indicates prograde transition from amphibolite to granulite facies conditions. **a** Initial Hbl-breakdown and first production of pyroxene grains, **b** Hbl free domains with recrystallizing pyroxene (left) and Hbl-replacement textures (right)

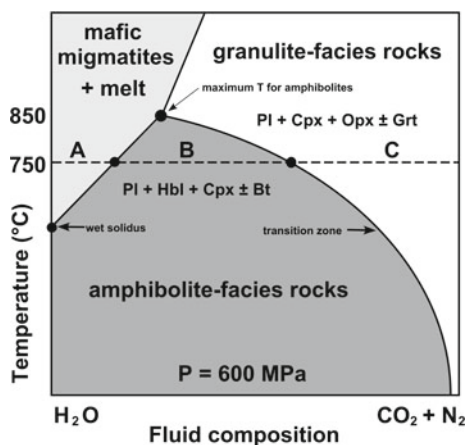
however, the overlap is smaller and the boundary between the two fields occurs close to 600–700 MPa at 800 °C.

Because high-grade brown hornblende is a rather stable mineral, very high temperatures are necessary to destroy this last hydrous phase in mafic rocks. Completely anhydrous mafic granulites normally form above 850 °C or at even higher temperatures. Amphibole dehydration is often aided by interaction of the rocks with an H₂O-poor external fluid phase. Alternatively, dehydration of amphibole may be triggered by partial melting and removal of H₂O by a melt phase

(see also Chap. 7 where general aspects of granulite facies metamorphism have been discussed). The relationships that are important in high-grade and granulite facies metamorphism of mafic rocks are shown in Fig. 9.17, which is a schematic T versus fluid composition diagram at an approximate P_{total} of 600 MPa. Along the 750 °C isotherm, three different assemblage fields are intersected. If H_2O -rich fluids are present (section A), mafic rocks undergo partial melting and mafic migmatites are formed (see Sect. 9.5.2). Intermediate fluid compositions are consistent with amphibolite facies rocks containing the typical assemblage: Pl + Hbl + Cpx (section B) and migmatite structures are absent. Fluids low in H_2O coexist with granulite facies rocks at the same T and the characteristic assemblage is: Pl + Cpx + Opx \pm Grt (section C). Note that the transition zone between the granulite and amphibolite facies assemblages in Fig. 9.17 extends over a wide range of fluid composition. However, an important conclusion from Fig. 9.17 is that at the same T (e.g. 750 °C) mafic migmatites, amphibolites and mafic granulites may be intimately associated in a metamorphic complex or terrain depending on the composition of a fluid phase. The situation may be complicated by variations of fluid composition over time at a particular site. Also note that the first melt in mafic rocks forms in the presence of a pure H_2O -fluid (wet solidus in Fig. 9.17). With increasing T , migmatites form with fluids that contain decreasing amounts of water. The amphibolite facies assemblage has a T -maximum that equates with an amphibole-out isograd at about 900 °C (at 600 MPa) in the presence of a pure H_2O -fluid. The T -maximum may be closer to 850 °C if mixed volatile fluids are present at the same pressure.

Although completely anhydrous mafic granulites are common, e.g., in the Jotun nappe and the Bergen arcs of the Scandinavian Caledonides, many mafic granulites still contain prograde hornblende (as opposed to retrograde post-granulite Hbl). A case in point is the amphibolite-granulite facies transition in metamafic rocks at Broken Hill, Australia. The color of Hbl changes with increasing grade from bluish-green through green-brown in amphibolite facies rocks to dark reddish brown in

Fig. 9.17 Schematic isobaric temperature versus fluid composition diagram showing amphibolite—granulite facies relationships in metamorphic mafic rocks



granulite facies rocks that mainly reflects increasing Ti (indication of increasing T). This is coupled with increasing Ed-substitution ($\text{Na}^{\text{A}}\text{Al}^{\text{A}}_{-1}\text{Si}_{-1}$). The presence of brown Hbl in mafic rocks that contain Opx defines a lower grade granulite facies; Hbl—two pyroxene granulite. The case is more difficult at high- P where Opx does not form in mafic rocks and the typical assemblage Pl + Cpx + Grt may also be present in the amphibolite facies or where Hbl persists to very high- T (1000 °C at 1.0 GPa). Obviously, in this case, the definition of the amphibolite—granulite facies **boundary** is impossible on the basis of mafic rocks alone (see comments in Chap. 4 on metamorphic grade).

An extreme case of garnet-amphibolite occurs at Gore Mountains in the Adirondack region of New York State (USA). The metamorphic mafic rocks formed at ultra-high- T granulite facies conditions estimated to $P \sim 1$ GPa and $T \sim 950$ °C (Shinewar et al. 2021). They contain extremely large pyrope-rich garnets (up to 40 cm large) and pargasitic hornblende in the matrix and tschermakitic hornblende rimming the garnets (Fig. 9.18). The rocks contain the assemblage Hbl + Pl + Grt + Opx \pm Qtz \pm Spl \pm Bt. The UHT amphibolites do not contain Cpx, which is very surprising. The two hydrates hornblende and biotite do not contain significant amounts of F or Cl that could replace OH thus stabilizing them at these very high T .

In addition to the minerals discussed so far, mafic granulites may also contain more exotic minerals such as sapphirine (Spr) or scapolite (Scp) in various assemblages. Also hercynitic spinel (Hc) is commonly present in mafic granulites and its presence is diagnostic of low- P conditions (<400 MPa).

At very low- P , such as represented by chemography #14 in Fig. 9.8, pyroxene hornfels forms by high- T contact metamorphism of mafic rocks. Ultimately, with UHT contact metamorphism of mafic rocks, the assemblage Pl + Cpx + Opx \pm Spl (chemography #14) will form that is identical to the basalt mineralogy shown in the upper left corner of Fig. 9.8. The upper boundary of granulite facies metamorphism of mafic rocks is given by the dry basalt liquidus at ~ 1200 °C.

The causes of granulite facies metamorphism at low- P are commonly attributed to intrusion of large volumes of dry or CO_2 -rich mafic (gabbroic/basaltic) or charnockitic magma to shallow crustal levels from the mantle or lower crust (see references for in this chapter and Chap. 7). The dry or CO_2 -rich nature of such magma facilitates dehydration of the crustal rocks and there is little tectonic activity associated with this type of granulite facies metamorphism. After heating to high- T , the granulite facies rocks cool essentially in-situ as evidenced by many granulite facies terrains being characterized by isobaric cooling paths (and perhaps a counter clockwise P - T loop; see also Chap. 3). In general, exhumation of granulite facies rocks requires a later contractional orogenic event that involves stacking and tilting of crustal slices with the formation of fold-nappe structures that ultimately permit the erosion surface to intersect middle or lower crust granulite terranes. If water becomes available during slow cooling, the high-grade assemblages may be completely erased and if Opx disappears from mafic granulites during amphibolitization it is very difficult to determine if the rocks were ever recrystallized under granulite facies conditions.



Fig. 9.18 Gore Mountain garnet amphibolite (Adirondacks, USA). Megacrystals of garnet in meta-gabbroic rocks formed at 1 GPa and ~950 °C. Assemblage: Grt + Pl + Hbl + Bt + Opx. Garnet contains 43 mol % pyrope component (Shinewar et al. 2021). Worlds largest garnets, up to 40 cm, no Cpx, no migmatite structures

9.7 Blueschist Facies Metamorphism

9.7.1 Introduction

Blueschists are rocks that contain a significant amount of blue alkali-amphibole with a very high proportion of Gln endmember component. Such rocks are, in an outcrop or hand specimen, blue in color. Note, however, that pure Gln is colorless under the microscope. If a rock contains a blue pleochroic amphibole in thin section it means that it is not a pure Gln and appreciable amounts of the riebeckite (Rbk) and other sodic ferro-ferric amphibole components are important and the overall composition of the amphibole is crossite (an amphibole name disapproved by IMA but still useful for petrologists). Note also that Cl-rich Hbl may have a blue color under the microscope. However, if metamafic rocks of basaltic bulk composition contain sodic amphibole, the rocks are likely to have been metamorphosed under the conditions of the blueschist facies.

The general P - T field of the blueschist facies is delineated in Fig. 4.3 and the blueschist facies mineralogy is represented by chemographies #16 and #17 in

Fig. 9.8. The lower P range is characterized by Gln (Na–Am) + Lws + Chl assemblages. In the higher-grade blueschist facies chemography #17, typical metamafic rocks contain various assemblages that include Gln (Na–Am), Zo (Czo–Ep), Grt, Pa, Phe, Chl, Tlc, Ky, Rt, Ank and other minerals.

A detailed rendering of the blueschist facies stability field is shown in Fig. 9.19. It is bounded towards the subgreenschist and greenschist facies by reactions 9.64, 9.65 and 9.66 in Table 9.2. The high- P boundary is given by reaction 9.71. Worldwide, blueschist facies terrains are associated with subduction zone metamorphism that typically occurs along destructive plate margins where basaltic oceanic crust is recycled to the mantle beneath the continental lithosphere. Two typical geotherms related to subduction tectonics are depicted in Fig. 9.19. The slow subduction geotherm only marginally passes through the blueschist field and eclogite assemblages are produced at pressures as low as 1.3 to 1.4 GPa. If subduction is fast, prominent blueschist facies terrains may develop and eclogite formation does not occur until pressures of 1.8 to 2.0 GPa are reached (corresponding to subduction depths of 50–60 km). Because there are natural limits to attainable subduction velocities in global tectonic processes, P – T conditions represented by

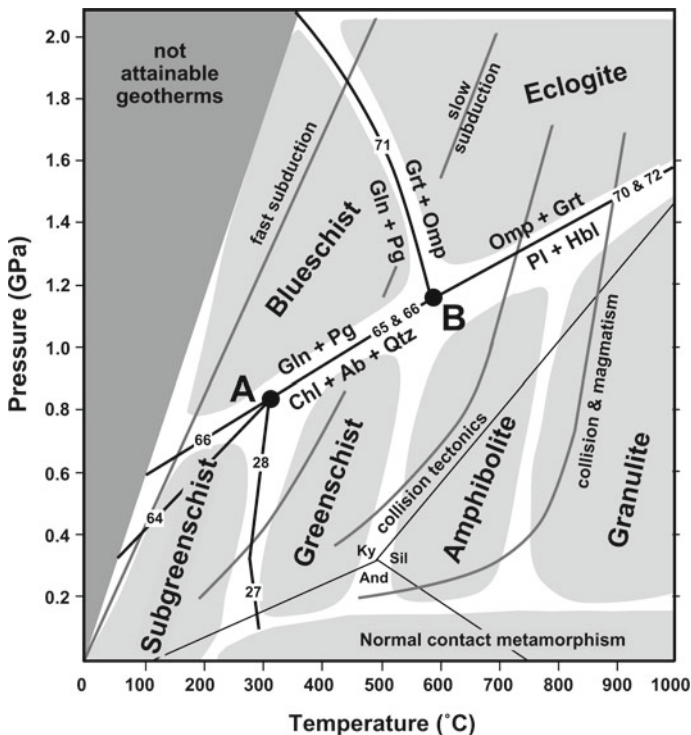


Fig. 9.19 Metamorphic facies scheme and reactions defining some of the field boundaries (reaction stoichiometry given on Table 9.2). The facies concept uses type assemblages of metabasaltic rocks (Chap. 4). Aluminosilicate phase transitions given for comparison

the upper left wedge area in Fig. 9.17 are conditions not accessible for metamorphism (but see discussion on “forbidden zone” in Chap. 6).

9.7.2 Reactions and Assemblages

As discussed above, reactions 9.27 and 9.28 mark the boundary between the subgreenschist facies and the greenschist facies. The boundary between subgreenschist facies and blueschist facies conditions is given by reaction 9.64. It replaces the low-grade assemblage Act + Chl + Ab by the high- P assemblage Gln + Lws. The reaction conserves H_2O and is formally independent of P_{H_2O} or fluid phase composition. Equilibrium of reaction 9.64 is shown in Fig. 9.17 for average mineral compositions found in low-grade equivalents of basaltic rocks.

Point A in Fig. 9.19 marks an important P - T region where blueschist, greenschist and subgreenschist facies assemblages meet at about 800 MPa and 300 °C. The P - T region is defined by the approximate intersection of the reactions 9.22, 9.28, 9.30, 9.31, 9.64, 9.66 and 9.70. Note, however, that point A is not an invariant point in Schreinemaker's sense but rather a relatively narrow P - T range of locations of various invariant points generated by the intersection of continuous reactions in the NCMASH system.

The blueschist facies is separated from the greenschist facies by reactions 9.65 and 9.66 shown in Fig. 9.19. Reaction 9.65 consumes the low-grade assemblage Chl + Act + Ab and replaces it by the most typical blueschist facies assemblage Gln + Ep (Zo). Reaction 9.65 connects points A and B in Fig. 9.19 and almost coincides with the other important reaction 9.66 that replaces the greenschist facies assemblage Chl + Ab by the characteristic blueschist assemblage Gln + Pg. If for any reason, some Ab should still be present in the rocks after all Chl is exhausted, it will be consumed by reaction 9.70. The boundary of reaction 9.66 is close to the heavy green boundary that separates a Pl-present from a Pl-absent region in Fig. 9.9. As in the eclogite facies, blueschists do not contain stable Ab (Pl). In most low-grade mafic rocks, however, Chl is much more abundant than is Ab and consequently, reactions 9.65 and 9.66 will normally remove it.

The Gln + Pg assemblage is replaced by Omp + Grt as a result of reaction 9.71. The reaction terminates the blueschist field towards higher P where it grades into the eclogite field with the diagnostic Omp + Grt assemblage. At low grade, the Na_2O present in metamafic rocks occurs in Ab, in the blueschist facies it is taken up by alkali-Am (Gln, crossite) and Pg, and in the eclogite facies it is stored in Na-Cpx (Omp, Jd). Reaction 9.71 has a negative slope on a P - T diagram (Fig. 9.19) and terminates at point B towards lower P where it becomes metastable relative to feldspar-involving reactions. The negative slope of reaction 9.71 means that the most favorable conditions for the development of extensive blueschist facies terranes are tectonic settings with fast subduction of cold (old) oceanic crust.

Inside the blueschist facies field, some additional reactions may modify the assemblages. Most important is reaction 9.67 that terminates the Lws + Gln assemblage represented by chemography #16 and produces Grt towards higher P

(chemography #17). Another important Grt-producing reaction in the blueschist facies is reaction 9.68. Reaction 9.69 generates the widespread Czo + Pg pseudomorphs that are diagnostic for the former presence of lawsonite in blueschists (see Sect. 9.2.1 and Fig. 9.10).

The continuous reactions within the blueschist facies field result in a systematic, gradual change in the mineral and modal composition of metabasaltic rocks during prograde metamorphism. For example, take a metabasaltic rock with a subgreenschist facies assemblage that undergoes subduction at a rate intermediate to the slow and fast subduction geotherms shown in Fig. 9.19. Such a geotherm will cover a T - P interval in the blueschist facies field from 250–500 °C and 0.7–1.6 GPa. At pressures between 600–800 MPa, Lws + Na–Am will begin to replace the low-grade Chl + Act + Ab assemblage. The first-formed Na–Am is initially fairly Fe-rich containing a significant Rbk-component. With a further increase in P , Ab gradually disappears and Am becomes increasingly sodic and depleted in the Act-component. In the M(4) site of the Am structure, Na replaces Ca by way of a Gln exchange mechanism $\text{Na}^{\text{M4}}\text{AlCa}^{\text{M4}}_{-1}\text{Mg}_{-1}$ that does not involve the amphibole A-site. The continuous reaction produces a Lws + crossite + Chl + Pa \pm Phe assemblage that is characteristic for pressures around 1.0 GPa. At still higher P , Lws gradually disappears; Na–Am becomes increasingly enriched in Gln-component, Czo and Ep become important members of the assemblages, while modal Chl continuously decreases. The characteristic assemblage for this intermediate blueschist facies stage is: Gln + Ep + Chl + Pg \pm Phe. Typical pressures for this assemblage are in the range of 1.2–1.4 GPa (along the fast subduction geotherm we are concerned with). With increasing P , Grt forms as a result of chlorite-involving reactions and high- P blueschists most typically contain Gln + Ep (Czo, Zo) + Grt + Pg \pm Phe. Other minerals that may be present in high- P /low- T blueschists include Mg–Cld, Tlc and Ky. For a discussion of systematic compositional changes in the only important potassic mineral in blueschists, Phe, with increasing P see Sect. 7.8. Also note that blueschists often contain carbonate minerals that give rise to mixed volatile reactions that are not discussed here. Blueschist carbonates include Cal and its high- P polymorph Arg, Ank, Dol, breunerite and Mgs. The origin of the carbonates is either related to ocean-floor metamorphism/metasomatism of basalt or they are derived from carbonate sediment deposited concurrently with the eruption of ocean floor basalt.

Blueschist facies assemblages are gradually replaced with the typical eclogite facies assemblage Omp + Grt at $P > \sim 1.4$ –1.6 GPa. Because high- P blueschists often contain Grt at these conditions, it is the appearance of Omp that marks the transition to eclogite facies conditions. The boundary is gradual and there is a wide P -range where Gln + Pa + Ep + Grt + Omp may occur as a stable association and strictly speaking, this assemblage is diagnostic for the eclogite facies. Along an intermediate high- P /low- T geotherm, typical eclogite assemblages are formed at about 1.6–1.8 GPa and a corresponding T of around 500 °C.

An example of progressive metamorphism from zeolite through prehnite-pumpellyite, blueschist to eclogite facies indicating a high- P low- T geotherm (0.2–1.4 GPa/100–540 °C) is the metabasite rocks of the Franciscan terrane, California. The

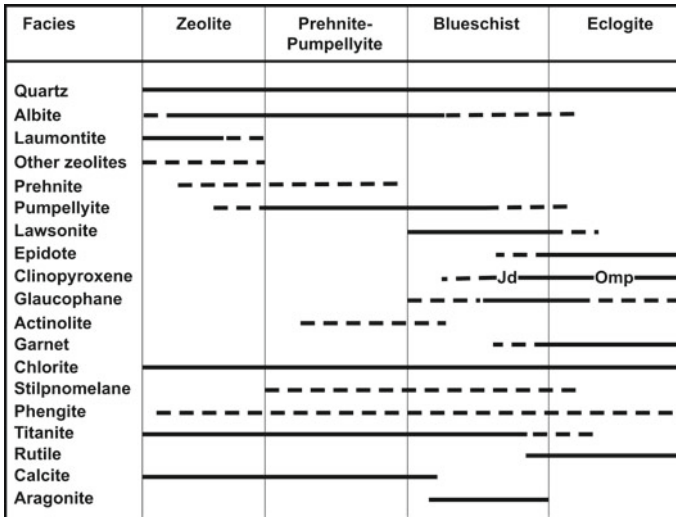


Fig. 9.20 Progressive mineral changes in high-*P* metabasites, Franciscan terrane, California. (data from Ernst 1965, 1971; Ernst et al. 1970; Jayko et al. 1986; Brothers and Grapes 1989)

sequence of mineral changes is shown in Fig. 9.20 and is constructed from assemblages in allochthonous metabasite fragments and eclogite “knockers” that occur throughout the greywacke–dominated subduction zone complex. Note that greenschist facies field is not intersected by the steep *P/T* trajectory and the typical greenschist facies minerals Act + Ab + Chl occur with Pmp and Prh. Blueschist facies metabasaltic rocks are characterized by the assemblage Qtz + Ab + Gln + Lws + Jd + Chl + Pmp + Ttn + Arg that also may include Phe and Stp and with Grt and Ep in the higher grade facies assemblage.

9.8 Eclogite Facies Metamorphism

9.8.1 Eclogites

Eclogites are metamorphic mafic rocks that contain the stable mineral pair **Grt** and **Omp** in significant amounts. Eclogites are free of Pl. Eclogites are very dense rocks with a density even greater than some ultramafic mantle rocks ($\rho_{\text{eclogite}} > 3300 \text{ kg m}^{-3}$) and because of this their origin can be readily related to very high-*P* conditions of formation. Omphacite + Grt is the diagnostic assemblage in metabasaltic rocks that recrystallized above about 1.2–1.4 GPa outside the stability field of Pl. Typical eclogites form at pressures of 1.8 to 2.2 GPa and higher. Many of the eclogites found in collisional mountain belts such as the Western Alps or the Scandinavian Caledonides still display clear compositional and structural evidence of being derived from basalt. In the Zermatt region of the Central Alps, for example,

preserved MORB compositions and pillow structures may be found in eclogites that formed at pressures greater than 2.5 GPa corresponding to a subduction depth of about 80 km. This is compelling evidence that surface rocks (basaltic lava) can be transported by active tectonic processes to depths of 80 km or more in the case of coesite-bearing eclogites found in UHP terranes.

The P - T field of the eclogite facies shown in Fig. 9.19 can be accessed in prograde metamorphism from all three neighboring facies fields, blueschist, amphibolite and granulite facies, depending on the tectonic setting. In subduction zones, eclogites originate from blueschists, as outlined above and these eclogite types often indicate very high- P formation.

In a continent–continent collision tectonic setting, the continental crust often attains twice its normal thickness and the deeper parts are exposed to pressures in the range of 1.2 to 2.4 GPa. Any mafic rocks of suitable composition in the deeper part of the thickened crust may be transformed to eclogite (Fig. 9.19). An example is the collision of the Eurasian and the Indian plates and the resulting formation of thickened crust underlying the Tibetan Plateau. Along a Ky-type geotherm, typical of collision tectonics shown in Fig. 9.19, eclogites will be created from amphibolites. Eclogites that form in such a tectonic setting characteristically record pressures in the range of 1.4 to 1.8 GPa rather than UHP.

If collision is accompanied by substantial magmatic heat transfer to the crust, eclogites may form from granulites along the “hot” geotherm in Fig. 9.19. Mantle-derived basaltic melts often sample rocks bordering conduits during their ascent to the surface. These fragments are found as xenoliths in basaltic lavas and include ultramafic rocks from the mantle, granulites from the lower crust and eclogites from a range of depths. The xenolith association is characteristic of abnormally hot geotherms caused by collision and magmatism, the initial stages of crustal extension or by magmatism alone. In such settings, eclogites may have been created from mafic granulites or directly crystallized from basaltic magma at great depth. Although the P -range of these high- T eclogites is very large, typical pressures are in the same range as those of eclogites formed from amphibolites. Basaltic magmas may also entrain eclogite xenoliths from great depth in the mantle but the ultimate origin of these deep eclogite samples is ambiguous and they could also represent fragments of recycled former oceanic crust.

From the comments above it follows that eclogites may form in a wide range of geotectonic settings and the eclogite facies comprises the widest P - T region of any of the metamorphic facies fields with a T -range from about 400 to 1000 °C. It also follows that three general types of eclogites can be distinguished depending on geological setting and formation- T .

1. **Low- T /high- P (LT/HP) eclogites** are related to subduction tectonics and form from blueschists. This type includes eclogites in UHP metamorphic terranes
2. Intermediate or **Medium- T (MT) eclogites** formed in continent collision double-crust settings from amphibolites
3. **High- T (HT) eclogites** formed in crustal extension settings where the geotherm is abnormally “hot” due to magmatic heat transfer from the mantle (e.g., basalt

magma underplating) from mafic granulites or have crystallized directly as eclogite from mafic magma.

The three different geodynamic types of eclogite are also characterized by typical mineral associations because of dramatically different temperatures and widely varying H_2O pressures associated with their formation. While LT/HP eclogites formed in subduction zones often contain modally large amounts of hydrate minerals, MT eclogites still contain assemblages with hydrates, typically zoisite-clinzoisite, HT eclogites often contain “dry” assemblages. Field examples of MT eclogites are shown in Fig. 9.21.

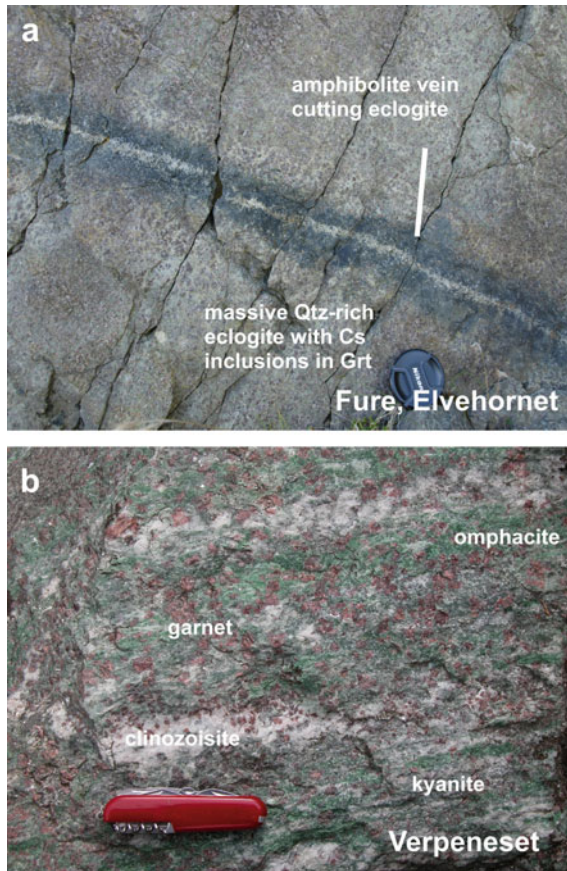


Fig. 9.21 Field examples of MT (HT) eclogites from classical eclogite outcrops in the Western Gneiss Region of Norway: **a** Coesite eclogite from Elvehornet, Fure, Stadlandet. Note dark amphibolitization vein cutting eclogite. **b** Verpeneset eclogite, outer Nordfjord (worlds most attractive eclogite outcrop!) with the typical MT assemblage: Omp + Grt + Czo + Ky + Qtz. **c** HT eclogite at the protected Gryting outcrop: Grt + Omp + Opx + Qtz. At the same outcrop Opx-free eclogite contains coesite as inclusions in Grt

In dealing with high- P rocks, important issues also include the mechanism by which they return to the surface, the P - T path of exhumation, and, most importantly, the modifications experienced by the rocks during decompression. For example, if an eclogite formed by subduction and equilibrated at 650 °C and 2.5 GPa, it is crucial for the fate of the eclogite assemblages whether the rocks reach the surface via the blueschist field (cooling and decompression occur simultaneously), via the amphibolite and greenschist fields (initial decompression and subsequent cooling), or via the granulite field (initial heating and decompression followed by cooling). Most eclogites display some indications of mineral reactions along their return paths. Access of H_2O along that return path is essential to whether or not the high- T assemblages are preserved or extensive retrogression occurs. On the other hand, as will be discussed below, LT/HP eclogites often contain abundant hydrate minerals such as Cld, Tlc, Czo at peak- P . Such rocks will undergo extensive dehydration reactions that will eventually eliminate the eclogite assemblage if decompression occurs without concurrent cooling.

9.8.2 Reactions and Assemblages

Reactions that connect the blueschist facies to **LT/HP eclogite facies** have been discussed in Sect. 9.7.2. The most typical assemblages in LT/HP eclogites involve the following minerals (bold = essential minerals): **Grt + Omp** \pm Czo \pm Cld \pm Phe \pm Pg \pm Gln \pm Qtz \pm Ky \pm Tlc \pm Rt \pm Dol. massive.

Omphacite is a sodic high- P clinopyroxene that is mainly composed of the components Jd, Acm, Di and Hd (a solid solution of: $NaAlSi_2O_6$ - $NaFe^{3+}Si_2O_6$ - $CaMgSi_2O_6$ - $CaFeSi_2O_6$). In typical Omp, the M(2) site of the pyroxene structure contains about 50% Na and 50% Ca. LT/HP eclogites often contain pure Jd together with Omp that commonly contains minor amounts of Cr giving the mineral a grass-green color, particularly in eclogitised metagabbros (Fig. 9.22). Note that Cr-Di in garnet-peridotite also shows a characteristic grass-green color. However, because ultramafic rocks contain very little sodium, the Jd-component in Cpx of high- P ultramafic rocks is generally very low.

Garnet in eclogite is a solid solution of the major phase components Alm, Prp and Grs, i.e. $Fe_3Al_2Si_3O_{12}$ - $Mg_3Al_2Si_3O_{12}$ - $Ca_3Al_2Si_3O_{12}$. However, due to its refractory nature, eclogite Grt can be inherited from earlier stages of metamorphism or be relics from the protolith, e.g. garnet-granulite.

In LT/HP eclogites, Cld is very Mg-rich and X_{Mg} may be as high as 0.9. Chloritoid and paragonite are diagnostic minerals in LT/HP eclogites. The two minerals are removed by various reactions at higher T so that they are typically absent in MT- and HT-eclogites.

Phengite and other sheet silicates that occur in LT/HP eclogites derived from gabbros also often contain small amounts of Cr giving them a green color, e.g. Cr-bearing Phe is termed fuchsite.

Ultrahigh- P eclogites, e.g. Western Alps, Bohemian Massif, Western Norway, Kokchetav Massif in Kazakhstan, Dabie Mountains and Sulu areas, China, are

indicated by the presence of coesite and even diamond in some cases, most often as inclusions in garnet and zircon.

9.8.2.1 Amphibolite and Granulite to Eclogite Facies Transition

Under eclogite facies conditions, the An-component of Pl in amphibolites and granulites is removed by reaction 9.72 and produces the Ca-Ts component in Omp. The equilibrium of reaction 9.72 is nearly T -independent and it can be used to estimate P . Reaction 9.73 that replaces An by Czo and Ky is the most important An-consuming reaction in high- P metamorphism of both MT- and HT-eclogites. The hydration reaction consumes H_2O but the absence of water will stabilize An. Nevertheless, if water is unavailable as a solvent then reaction kinetics are so slow and transport distances so small that Ab and other low- P phases or phase components can survive to high- P . For example, in olivine gabbros of the Zermatt-Saas nappe (Western Alps, see below) primary igneous minerals have survived pressures in excess of 2.0 GPa at around 600 °C without forming eclogite except where water has had access to the rocks. Another example is the Precambrian mafic granulites of the Bergen Arcs (Norwegian Caledonides), a basement nappe complex that experienced $P \sim 2.0$ GPa and $T \sim 700$ °C during Caledonian metamorphism. In this case, mafic granulite is perfectly preserved over large areas (Fig. 9.1b) except along an anastomosing network of shears that permitted access of water to produce an MT eclogite assemblage.

The equilibrium conditions of reaction 9.73 shown in Fig. 9.19 indicate that it is approximately parallel to the Ab-breakdown reaction 9.70. Reaction 9.74 decomposes the An-component in Pl and produces a Grs-component in eclogite garnet together with kyanite and quartz. The slope of the reaction is similar to those of reactions 9.70 and 9.72 (Fig. 9.19).

Reaction 9.70 has been used in Chap. 3 to illustrate some general principles of chemical reactions in rocks. In high- P mafic rocks it is the most important reaction as it delineates the boundary between a Pl-present and a Pl-absent region in P - T space (Fig. 9.19). If all three minerals are present (Qtz, Pl and Na-Cpx), the equilibrium conditions of reaction 9.70 can be used for P -estimates if T can be determined from a geothermometer such as Fe-Mg distribution between Grt and Omp. In the absence of Qtz, maximum P can be estimated from the pyroxene-feldspar pair. If feldspar is not present (the normal case in eclogites), the Omp + Qtz assemblage can be used to estimate a minimum P for eclogite formation assuming unit activity for the Ab-component in the equilibrium constant expression for reaction 9.70. Other important reactions of the amphibolite (or granulite) to eclogite transition zone must consume Cam or Cpx. An example is reaction 9.75 that destroys Tr- and the An-component ($Hbl + Pl = \text{amphibolite}$) and produces Grt + Cpx. Reactions 9.76, 9.77, and 9.78 are examples of An-consuming reactions relevant for the transition from the granulite to HT-eclogite facies rocks.

As a result of the reactions that produce **MT-eclogites (from amphibolites)** the typical minerals found in meta-MORB are: **Grt + Omp** \pm Zo (Czo) \pm Phe \pm Ky \pm Am (Na-Cam) \pm Qtz (Cs at UHP) \pm Rt.

High-T eclogites (from granulites) typically contain: **Grt + Omp** \pm Ky \pm Opx \pm Am \pm Qtz (Cs at UHP) \pm Rt.

9.8.2.2 Reactions in Eclogites

Prograde metamorphic mineral reactions that affect eclogites are basically ordinary dehydration reactions. The reactions transform assemblages involving hydrous minerals of LT/HP-eclogites and substitute them with less hydrous assemblages of MT-eclogites and ultimately HT-eclogites. Examples are the Pg breakdown reaction 9.79, the Czo breakdown reaction 9.80, and the replacement of Tlc + Ky by Opx reaction 9.81. Other reactions gradually remove Chl from Qtz-free MT-eclogites, some of them producing Opx. Reaction 9.80 replaces Czo and Grt to produce Ky + Cpx. This continuous reaction relates MT- to HT-eclogites and the reaction ultimately leads to the change from chemography #18 to #19 in Fig. 9.8.

Other important reactions in HT-eclogites are 9.82 and 9.83. The latter reaction is important in relatively rare Opx-bearing eclogites, e.g. eclogites of the Western Gneiss region of the Scandinavian Caledonides. Phengite is the only K-bearing phase in LT/HP-eclogites. At higher T the mica continuously decomposes to produce a K-amphibole component. K-bearing Na–Ca-amphiboles found in high-grade eclogites are very stable and remain the prime K-carrier in HT-eclogites.

9.8.3 Eclogite Facies in Gabbroic Rocks

Mafic rocks cover a wide range in bulk composition. Eclogite with Grt and Omp as the dominant minerals usually develop from basaltic protoliths. The above discussion refers to MORB-type basaltic eclogite, but many gabbros are compositionally dissimilar to MORB. In particular, gabbros are commonly much more Mg- (or Fe-rich = ferrogabbro) compared to MORB and it can be expected that high-*P* equivalents of troctolite and olivine-gabbro may develop mineral assemblages that are quite different from normal basaltic eclogite facies Grt + Omp rocks. In fact, Mg-rich olivine gabbro metamorphosed at 2.5 GPa and 600 °C may not contain Grt + Omp as a peak assemblage because the low X_{Fe} of Mg-gabbro protoliths prevents the formation of Grt. An example of LT/HP-eclogite metamorphism of an olivine gabbro from the Western Alps is presented in Sect. 9.8.2.1 below. Although such mafic rocks have been metamorphosed under eclogite facies conditions, they are not strictly eclogites, i.e. mafic eclogites. We also recommend avoiding rock names like pelitic eclogites or pelitic blueschists. The appropriate expressions for such rocks are blueschist facies metapelites or eclogite facies pelitic gneisses (see Sect. 7.7).

Anorthosites, which are also basic rocks, cannot be converted to eclogites by high-*P* metamorphism because the rocks contain more than 90–95% Pl. Plagioclase of the composition An_{70} will be converted into a Jd + Zo + Ky + Qtz assemblage under LT/HP and MT eclogite facies conditions (see Fig. 9.9).

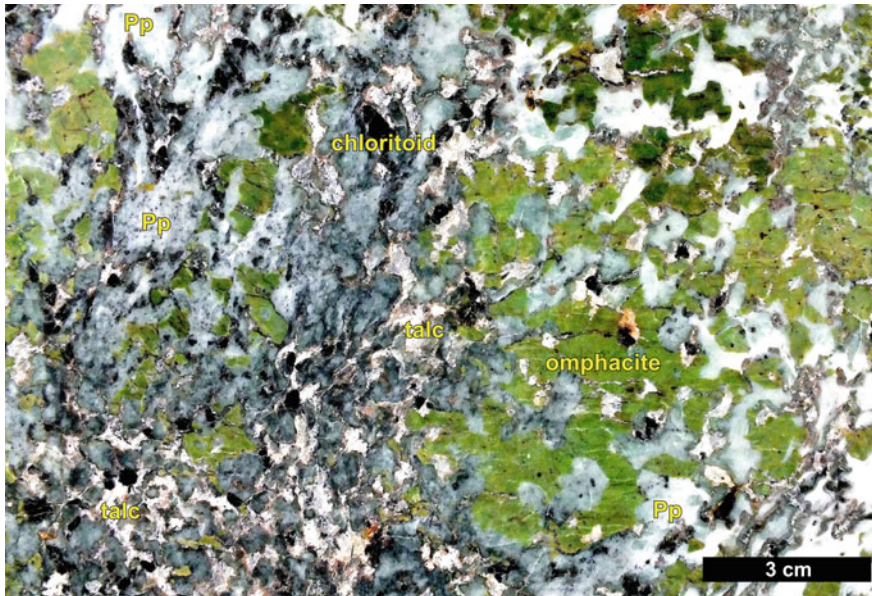


Fig. 9.22 Polished slab of eclogite facies Allalin gabbro (Zermatt-Saas nappe, Western Alps). The protolith gabbro contained the assemblage $Pl + Cpx + Ol$. Eclogite-facies hydration replaced Ol by $Tlc + Cld$ ($Tlc = white$, $Cld = black$), Cpx (augite) by Omp ($Omp = green$), and Pl by ultra-fine-grained glossy domains consisting of $Jd + Zo + Ky + Qtz$ ($Pp = plagioclase pseudomorphs$)

9.8.3.1 Blueschist and Eclogite Facies Metamorphism of Olivine Gabbro

A 2×5 km block of gabbro that forms the Allalinhorn (a 4027 m high peak) between Zermatt and Saas, Western Alps, Switzerland, it is referred to as the Allalin gabbro (Bearth 1967; Chinner and Dixon 1973; Meyer 1983a, b). The gabbro occurs within a typical metamorphic ophiolite complex (Zermatt-Saas ophiolite) that represents the oceanic lithosphere of the Mesozoic Tethys Ocean. During early Tertiary Alpine orogeny, the ophiolites and the Allalin gabbro were subducted to 80–100 km depth and metamorphosed under LT/HP eclogite facies conditions. Pillow basalts were converted to ordinary LT/HP eclogites, later retrogressed to blueschists, and finally overprinted by greenschist facies metamorphism. Abundant eclogite Grt represents the only relic mineral from the eclogite stage in locally strongly retrogressed eclogites and Grt -bearing greenschists demonstrate the refractory nature of the Grt .

The Allalin gabbro is an Mg-rich olivine gabbro with irregular layers of troctolite. The gabbro probably formed at the crust-mantle boundary beneath the continental crust south of the Tethys during the Jurassic where it underwent granulite facies recrystallization prior to being incorporated in the Tethys ophiolite during subduction (Bucher and Grapes 2009). The LT/HP metamorphism converted the gabbro mostly to an eclogite facies meta-gabbro (Fig. 9.22) leaving locally

some relics of the igneous protolith. The most prominent “peak” rock (Fig. 9.22) experienced extremely variable degrees of retrogression in irregular domains of the outcrop. The succession of minerals that formed in the gabbro through its entire P – T history is given in Fig. 9.23 and the P – T path from magmatic crystallization, through granulite facies conditions to peak eclogite facies (return point) and retrograde eclogite, amphibolite and amphibolite-greenschist transition facies is shown in Fig. 9.24. The metamorphic history of the gabbro can be subdivided into various stages: (A) Crystallization of a gabbroic Pl + Ol + Cpx + Ilm assemblage. These igneous minerals have survived subsequent metamorphism in undeformed areas of the rocks where H₂O never had access; (B) Recrystallization during final cooling under granulite facies conditions caused by crustal thickening to form Opx and Grt (as corona minerals between Ol and Pl) at ~850 °C/0.8–1.0 GPa). (C) Entrainment of the gabbro in subducting ophiolitic rocks and first hydration to form Chl that partly replaces Ol, Opx and Cpx. Chl forms part of the Opx + Grt coronas instead of Spl that would normally have formed under anhydrous granulite facies conditions; (D) Replacement of Pl by a Jd + Omp + Czo + Ky + Qtz assemblage indicating early stage eclogite facies conditions followed by Omp + Tlc + Rt after Cpx and Tlc + Cld + Ky after Ol and with corona Grt remaining stable, indicating peak eclogite facies conditions at 2.5–2.6 GPa and ~600 °C (Fig. 9.24). The key property of the LT/HP eclogitic gabbro is the occurrence of a number of hydrous phases (Tlc, Cld, Zo-Czo ± Chl) indicating that it owes its existence to the access of water during subduction; (E) A highest- P retrograde blueschist facies stage is characterized by the formation of Gln, Pg, Phe that replace Omp and Cld in parts of the rocks where deformation was more intense and access of water occurred; (F) At lower- P , the rocks entered the transitional facies between blueschist and greenschist with the formation of symplectites that replace the eclogite facies minerals, i.e., barroisite + Na-Cpx + Ab + oligoclase + Chl after Omp, Mrg + Pg + preiswerkite after chloritoid, and Ab + barroisite after Gln. These assemblages are fine-grained reaction products of local hydration; (G) Greenschist facies recrystallisation resulted from the return to shallower depths and the formation of Act + Bt + Ab + Chl + Ep at ~400–500 MPa and 400–450 °C. The late Alpine greenschist facies overprint is accompanied by two distinct phases of deformation. The impact of these stages on the Allalin gabbro varies from place to place and ranges from virtually nothing to complete retrogression. The greenschist facies deformation and hydration is often localized along shear zones and deformation is ductile in contrast to the eclogite-stage deformation that has been brittle. (H) Subgreenschist facies minerals, Ab, Cal, Prh, are mainly found in veins. The Allalin gabbro also contains sulfides, oxides and other accessory minerals such as Ttn, Crn and Dsp, that were stable at various stages of the P – T history of the rock.

The example of the Allalin gabbro provides a complex mineral reaction history. Successive development of minerals and mineral assemblages indicate that:

- Deformation is essential in metamorphic processes. It allows water to enter dry igneous rocks. In the absence of water, igneous and metamorphic assemblages

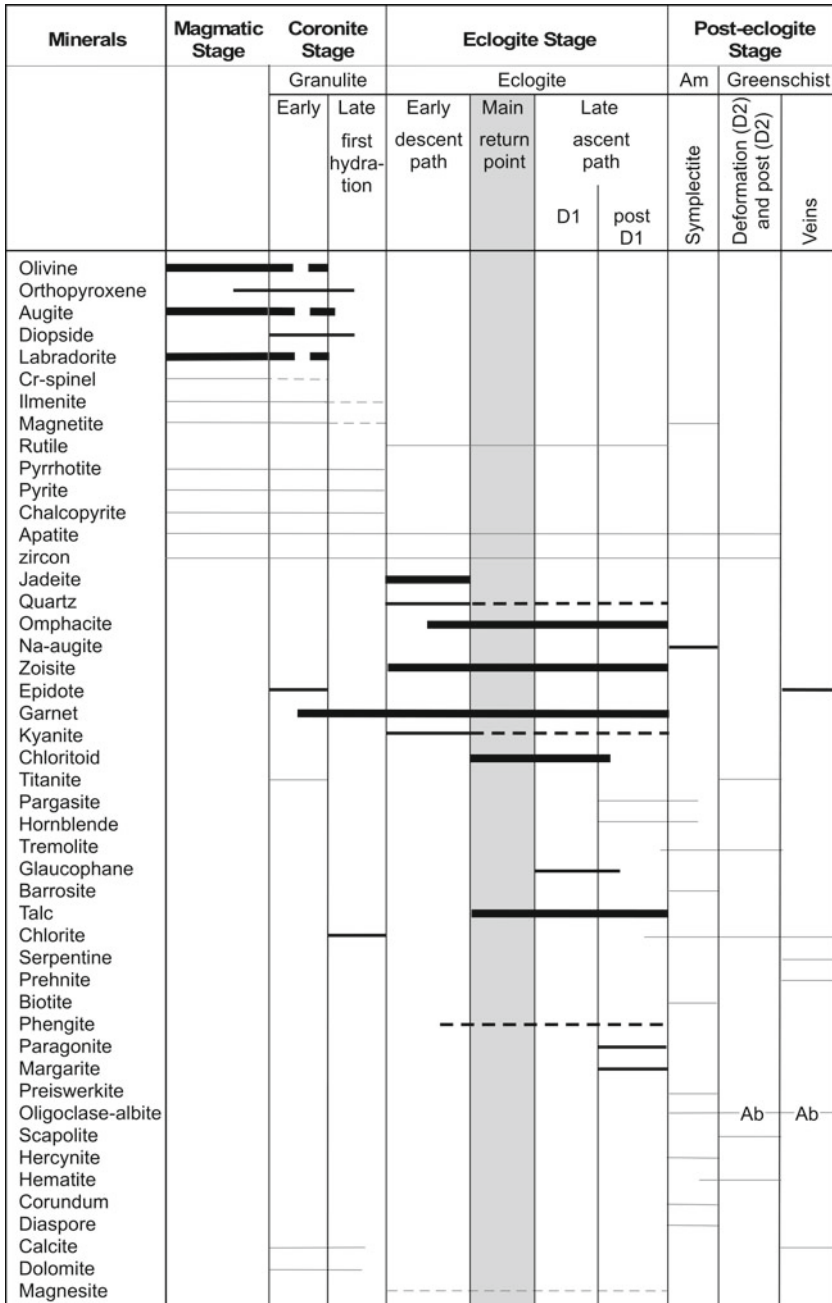


Fig. 9.23 Minerals versus time table of Allalin gabbro along the P - T - t path shown in Fig. 9.24 (after Bucher and Grapes 2009). Heavy lines = major minerals, regular lines = minor minerals, thin lines = accessory minerals, dashed lines = rare occurrence

will survive under extreme P - T conditions (e.g., igneous Pl + Cpx + Ol at 2.5 GPa and 600 °C).

- Mafic rocks that undergo eclogite facies metamorphism do not necessarily become eclogites. The bulk composition of many gabbros may not be favorable for the formation of modal abundant Grt.
- LT eclogite facies mafic rocks that form by subduction of oceanic lithosphere, are characterized by the presence of a number of hydrous minerals at peak- P conditions of the eclogite facies (Zo, Cld, Tlc, Chl, Phe).
- LT eclogite facies rocks may pass through the blueschist facies on their return path to the surface. The blueschist facies overprint is then retrograde in nature and adds another group of hydrous minerals such as Gln and Pg to the high- P /low- T assemblage.
- All stages of the complex P - T path followed by the Allalin gabbro and the reaction history involving a large number of minerals may be preserved in a single rock body. The predominant assemblage that is found in a single hand specimen or within a small area of a given outcrop depends on how much water entered the rock at a given P - T stage in its metamorphic evolution.
- The availability of water is in turn related to the local extent and nature of deformation. Given a certain stage, if much water is available, the formation of the maximum hydrated assemblage for that stage is possible. Water is consumed by hydration reactions that tend to dry out the rock. Thus, water must be continuously supplied in order to facilitate reactions that produce the maximum hydrated assemblage of that stage. Access for water to the originally dry rock is provided by micro-fractures and other brittle deformation structures during high- P metamorphism and by pervasive ductile deformation during greenschist facies metamorphism.

Some of these relationships are well visible using XRF images of polished rock slabs from Allalin gabbro (Fig. 9.25). The image has been taken from a slab similar to the one shown on Fig. 9.22. The rock shows the state at the maximum P and alpine T conditions at the return point of the subduction process (Fig. 9.24). The image shows the distribution of Cr (green), Fe (red) and Ni (blue). The green Cr signal marks the location of green Cr-bearing omphacite. The omphacite developed from and now pseudomorphs igneous augite. It is also evident that there was very limited or no ductile deformation along the path from A to D shown on Fig. 9.24. The blue Ni signal originates from the talc patches pseudomorphing igneous olivine containing minor amounts of Ni (~0.2 wt.%). The red Fe signal derives from garnet coronas around igneous olivine. The black zones between Tlc and Grt are Opx formed during the corona stage (stage B Fig. 9.24). The original sequence under granulite facies conditions was: Pl-Grt-Opx-Ol. Later during subduction Ol was hydrated to Tlc but the local structure was preserved and Ni remained at the original Ol location. Some Tlc patches inside Omp do not show Grt-Opx coronas because Pl did not “see” the hidden Ol. Finally, the black regions in Fig. 9.25 labeled Pp are the fine-grained plagioclase pseudomorphs consisting of Jd-Zo-Ky-Qtz described in the text above.

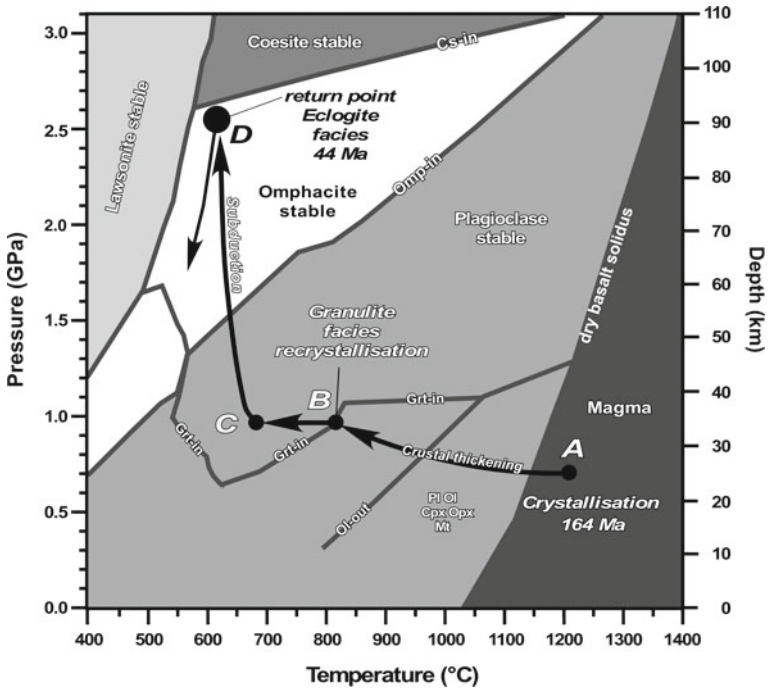


Fig. 9.24 Prograde and retrograde P - T - t paths (arrowed solid lines) of the Allalin gabbro (Swiss Alps) shown in relation to stages A: igneous crystallization, B: granulite facies, C: first hydration reactions, D: main eclogite facies stage given in the mineral table (Fig. 9.23) and discussed in text (after Bucher and Grapes 2009). Note: Crystallization depth of gabbro at 25 km depth (not oceanic)

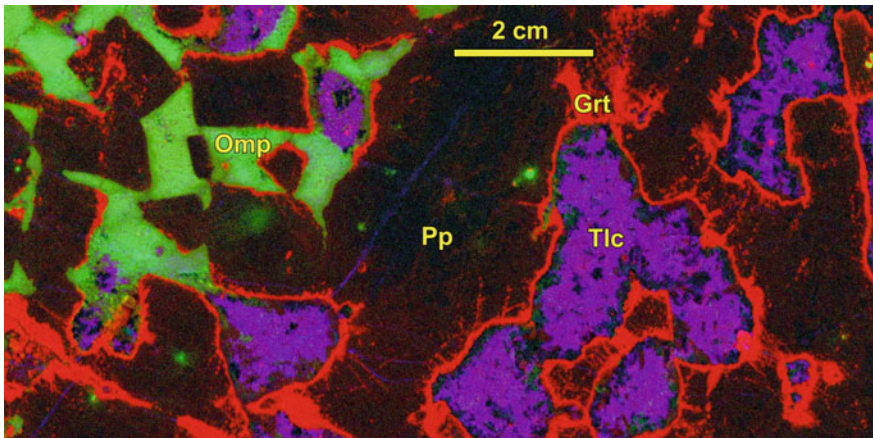


Fig. 9.25 XRF Image of a polished slab of Allalin gabbro (Fig. 9.22). It represents the state of the rock at its return point (maximum alpine P and T). Chromium in green, iron in red and nickel in blue (see text). Green: Omphacite, Red: Garnet, Blue: Talc. Very bright green spots: Cr-spinel. Image kindly taken on a μ XRF instrument at the University of Halle (Saale) by Rüdiger Kilian

The Allalin gabbro example shows that element distribution images taken by the μ XRF can be a very helpful tool that help unraveling complex reaction histories of rock samples. It is strongly recommended to generate element distribution maps with the μ XRF from your most complex samples of metamorphic rocks in addition to the standard microscopy and EPMA work. The Allalin gabbro is furthermore an excellent example of a rock with a complex reaction history that never reached a full overall chemical equilibrium (except for the very early magmatic crystallization perhaps). It also shows that a meaningful geologic evolution can be derived from these nonequilibrium rocks.

References

Cited References

- Arnórsson S (1995) Geothermal systems in Iceland; structure and conceptual models; I. High-temperature area. *Geothermics* 24:561–602
- Bearth P (1967) Die Ophiolithe der Zone von Zermatt-Sass-Fee. *Beiträge zur Geologischen Karte der Schweiz* 132 NF:130
- Boles JR, Coombs DS (1975) Mineral reactions in zeolitic Triassic tuff, Hokonui Hills, New Zealand. *Geol Soc Am Bull* 86:163–173
- Brothers RN, Grapes RH (1989) Clastic lawsonite, glaucophane and jadeitic pyroxene in Franciscan metagraywackes from the Diablo Range, California. *Geol Soc Am Bull* 101:14–26
- Bucher K, Fazines Y, De Capitani C, Grapes R (2005) Blueschists, eclogites, and decompression assemblages of the Zermatt-Saas ophiolite: high-pressure metamorphism of subducted Tethys lithosphere. *Am Mineral* 90:821–835
- Bucher K, Frost BR (2006) Fluid transfer in high-grade metamorphic terrains intruded by anorogenic granites: the Thor Range, Antarctica. *J Petrol* 47:567–593
- Bucher K, Grapes R (2009) The Allalin gabbro of the Zermatt-Saas ophiolite, Western Alps: a record of subduction zone hydration. *J Petrol* 50:1405–1442
- Carmichael RS (1989) Practical handbook of physical properties of rocks and minerals. CRC Press, Boca Raton, p 834
- Chinner GA, Dixon JE (1973) Some high-pressure parageneses of the Allalin gabbro, Valais, Switzerland. *J Petrol* 14:185–202
- Cho M, Liou JG, Maruyama S (1986) Transition from the zeolite to prehnite-pumpellyite facies in the Karmutsen metabasites, Vancouver island, British Columbia. *J Petrol* 27:467–494
- Cho M, Liou JG (1987) Prehnite-pumpellyite to greenschist facies transition in the Karmutsen metabasites, Vancouver island, B.C. *J Petrol* 28:417–443
- Ernst WG (1965) Mineral paragenesis in Franciscan metamorphic rocks, Panoche Pass, California. *Geol Soc Am Bull* 76:879–914
- Ernst WG (1971) Do mineral paragenesis reflect unusually high-pressure conditions in Franciscan metamorphism? *Am J Sci* 271:81–108
- Ernst WG, Seki Y, Onuki H, Gilbert MC (1970) Comparative study of low-grade metamorphism in the California Coast Ranges and the Outer Metamorphic Belt of Japan. *Geol Soc Am Mem* 124:276p
- Hollocher K (1991) Prograde amphibole dehydration reactions during high-grade regional metamorphism, Central Massachusetts, U.S.A. *Am Mineral* 76:956–970

- James HL (1955) Zones of regional metamorphism in the Precambrian of northern Michigan. *Geol Soc Am Bull* 66:1455–1488
- Jayko AS, Blake MC, Brothers RN (1986) Blueschist metamorphism of the Eastern Franciscan belt, northern California. In: Evans BW, Brown EH (eds) *Blueschists and eclogites*. Geological Society of America Memoir, vol 164, pp 107–123
- Kuniyoshi S, Liou JG (1976) Burial metamorphism of the Karmutsen volcanic rocks, northeastern Vancouver Island, British Columbia. *Am J Sci* 276:1096–1119
- Liou JG, Maruyama S, Cho M (1987) Very low-grade metamorphism of volcanic and volcanoclastic rocks—mineral assemblages and mineral facies. In: Frey M (ed) *Low temperature metamorphism*. Blackie, Glasgow, pp 59–113
- Meyer J (1983a). *Mineralogie und Petrologie des Allalingsabbros*. Doctoral dissertation, University of Basel, p 329
- Meyer J (1983b). The development of the high-pressure metamorphism in the Allalin metagabbro (Switzerland). *Terra Cognita* 3:187 (Abs)
- Seki Y, Oki Y, Matsuda T, Mikami K, Okumura K (1969) Metamorphism in the Tanzawa Mountains, central Japan. *J Japan Ass Mineral Petrol Econ Geol* 61(1–29):50–75
- Shinevar WJ, Jagoutz O, VanTongeren JA (2021) Gore mountain garnet amphibolite records UHT conditions: implications for the rheology of the lower continental crust during orogenesis. *J Petrology* 62(4):1–28
- Weisenberger T, Bucher K (2010) Zeolites in fissures of granites and gneisses of the Central Alps. *J Metamorph Geol* 28:825–847

Further Reading and Additional Literature

- Mj A, Liou JG (1983) Phase relations amongst greenschist, epidote-amphibolite, and amphibolite in a basaltic system. *Am J Sci* 283A:328–354
- Austrheim H, Griffin WL (1985) Shear deformation and eclogite formation within granulite—facies anorthosites of the Bergen Arcs, Western Norway. *Chem Geol* 50:267–281
- Auzanneau E, Schmidt MW, Vielzeuf D, Connolly JAD (2010) Titanium in phengite: a geobarometer for high temperature eclogites. *Contrib Miner Petrol* 159:1–24
- Banno S (1986) The high pressure metamorphic belts in Japan: a review. *Geol Soc Am Mem* 164:365–374
- Barnicoat AC, Cartwright I (1997) The gabbro-eclogite transformation: an oxygen isotope and petrographic study of west Alpine ophiolites. *J Metamorph Geol* 15:93–104
- Bevins RE, Robinson D (1993) Parageneses of Ordovician sub-greenschist to greenschist facies metabasites from Wales, U.K. *Eur J Mineral* 5:925–935
- Bohlen SB, Liotta JJ (1986) A barometer for garnet amphibolites and garnet granulites. *J Petrol* 27:1025–1034
- Brothers RN, Yokoyama K (1982) Comparison of high pressure schists belts of New Caledonia and Sanbagawa, Japan. *Contrib Mineral Petrol* 79:219–229
- Brovarone AV (2014) Lawsonite: a delicate, yet fundamental mineral at HP–LT conditions. *J Metamorphic Geol* 32:435–436
- Brown EH (1974) Comparison of the mineralogy and phase relations of blueschists from the North Cascades, Washington and greenschists from Otago, New Zealand. *Geol Soc Am Bull* 85:333–344
- Brown EH (1977) The crossite content of Ca-amphibole as a guide to pressure of metamorphism. *J Petrol* 18:53–72
- Bucher K, Weisenberger T (2013) Fluid induced mineral composition adjustments during exhumation: the case of Alpine stilbite. *Contrib Miner Petrol* 166:1489–1503
- Chapman T, Clarke GL (2020) Cryptic evidence for the former presence of lawsonite in blueschist and eclogite. *J Metamorphic Geology* 39:343–362

- Cheng N, Jenkins DM (2019) Experimental study of metamorphic reactions and dehydration processes at the blueschist–eclogite transition during warm subduction. *J Metamorphic Geology* 39:39–56
- Coleman RG, Lee DE, Beatty LB, Brannock WW (1965) Eclogites and eclogites: their differences and similarities. *Geol Soc Am Bull* 76:483–508
- Coombs DS, Ellis AJ, Fyfe WS, Taylor AM (1959) The zeolite facies, with comments on the interpretation of hydrothermal syntheses. *Geochim Cosmochim Acta* 17:53–107
- Cooper AF (1972) Progressive metamorphism of metabasic rocks from the Haast Schist group of southern New Zealand. *J Petrol* 13:457–492
- Cox RA, Indares A (1999) Transformation of Fe-Ti gabbro to coronite, eclogite and amphibolite in the Baie du Nord segment, Maicouagan Imbricate Zone, eastern Grenville Province. *J Metamorph Geol* 17:537–555
- Davis PB, Whitney DL (2006) Petrogenesis of lawsonite and epidote eclogite and blueschist, Sivrihisar Massif, Turkey. *J Metamorph Geol* 24:823–849
- de Paoli MC, Clarke GL, Klepeis KA, Allibone AH, Turnbull IM (2009) The eclogite-granulite transition: Mafic and intermediate assemblages at breaksea sound, New Zealand. *J Petrol* 50:2307–2344
- El-Shazly AK (1994) Petrology of lawsonite-, pumpellyite- and sodic amphibole-bearing metabasites from north-east Oman. *J Metamorph Geol* 12:23–48
- Elmer FL, White RW, Powell R (2006) Devolatilization of metabasic rocks during greenschist–amphibolite facies metamorphism. *J Metamorph Geol* 24:497–513
- Eskola P (1921) On the eclogites of Norway. *Skr. Vidensk. Selsk. Christiania, Mat.-nat Kl. I* 8:1–118
- Evans BW (1990) Phase relations of epidote-blueschists. *Lithos* 25:3–23
- Evans BW, Brown EH (1986) Blueschists and eclogites. *Geol Soc America Mem. The Geological Society of America, Boulder, Colorado*, p 423
- Ferry JM (1984) Phase composition as a measure of reaction progress and an experimental model for the high-temperature metamorphism of mafic igneous rocks. *Am Mineral* 69:677–691
- Forbes RB, Evans BW, Thurston SP (1984) Regional progressive high-pressure metamorphism, Seward peninsula, Alaska. *J Metamorph Geol* 2:43–54
- Frederico L, Capponi G, Crispini L, Scambelluri M (2004) Exhumation of alpine high-pressure rocks: insights from petrology of eclogite clasts in the Tertiary Piedmontese basin (Ligurian Alps, Italy). *Lithos* 74:21–40
- Frey M, De Capitani C, Liou JG (1991) A new petrogenetic grid for low-grade metabasites. *J Metamorph Geol* 9:497–509
- Griffin WL, Austrheim H, Brastad K, Bryhni I, Krill A, Mørk MBE, Qvale H, Tørudbakken B (1983) High-pressure metamorphism in the scandinavian caledonides. In: Gee DG, Sturt BA (eds) *The caledonide orogen—scandinavia and related areas*, Wiley, Chichester
- Hamelin C, Brady JB, Cheney JT, Schumacher JC, Able LM, Sperry AJ (2018) Pseudomorphs after Lawsonite from Syros, Greece. *J Petrol* 59:2353–2384
- Harte B, Graham CM (1975) The graphical analysis of greenschist to amphibolite facies mineral assemblages in metabasites. *J Petrol* 16:347–370
- Hartel THD, Pattison DRM (1996) Genesis of the Kapsuskasing (Ontario) migmatitic mafic granulites by dehydration melting of amphibolite: the importance of quartz to reaction progress. *J Metamorph Geol* 14:591–611
- Heinrich CA (1986) Eclogite facies regional metamorphism of hydrous mafic rocks in the central Alpine Adula Nappe. *J Petrol* 27:123–154
- Helms TS, McSween HY Jr, Labotka TC, Jarosewich E (1987) Petrology of a Georgia Blue ridge amphibolite unit with hornblende + gedrite + kyanite + staurolite. *Am Mineral* 72:1086–1096
- Hirajima T, Banno S, Hiroi Y, Ohta Y (1988) Phase petrology of eclogites and related rocks from the Motalafjella high-pressure metamorphic complex in Spitsbergen (Arctic Ocean) and its significance. *Lithos* 22:75–97

- Hirajima T, Hiroi Y, Ohta Y (1984) Lawsonite and pumpellyite from the Vestgotabreen Formation in Spitsbergen. *Norsk Geol Tidsskrift* 4:267–273
- Holland TJB (1979) High water activities in the generation of high pressure kyanite eclogites of the Tauern Window, Austria. *J Geol* 87:1–27
- Holland TJB, Richardson SW (1979) Amphibole zonation in metabasites as a guide to the evolution of metamorphic conditions. *Contrib Mineral Petrol* 70:143–148
- Hosotani H, Banno S (1986) Amphibole composition as an indicator of subtle grade variation in epidote-glaucophane schists. *J Metamorph Geol* 4:23–36
- Humphris SE, Thompson G (1978) Hydrothermal alteration of oceanic basalts by seawater. *Geochim Cosmochim Acta* 42:107–125
- Johnson CD, Carlson WD (1990) The origin of olivine-plagioclase coronas in metagabbros from the Adirondack Mountains, New York. *J Metamorph Geol* 8:697–717
- Kawachi Y (1975) Pumpellyite-actinolite and contiguous facies metamorphism in the Upper Wakatipu district, southern New Zealand. *NZ J Geol Geophys* 17:169–208
- Konzett J, Hoinkes G (1996) Paragonite-hornblende assemblages and their petrological significance: an example from the Austroalpine Schneeberg Complex, Southern Tyrol, Italy. *J Metamorph Geol* 14:85–101
- Krogh Ravna EJ, Terry MP (2004) Geothermobarometry of UHP and HP eclogites and schists—an evaluation of equilibria among garnet-clinopyroxene-kyanite-phengite-coesite/quartz. *J Metamorph Geol* 22:593–604
- Laird J (1980) Phase equilibria in mafic schist from Vermont. *J Petrol* 21:1–27
- Laird J, Albee AL (1981) High pressure metamorphism in mafic schist from northern Vermont. *Am J Sci* 281:97–126
- Liogys VA, Jenkins DM (2000) Hornblende geothermometry of amphibolite layers of the Popple Hill gneiss, north-west Adirondack Lowlands, New York, USA. *J Metamorph Geol* 18:513–530
- Liou JG, Maruyama S, Cho M (1985) Phase equilibria and mineral paragenesis of metabasites in low-grade metamorphism. *Mineral Mag* 49:321–333
- Liu X, Wei C, Li S, Dong S, Liu J (2004) Thermobaric structure of a traverse across western Dabieshan: implications for collision tectonics between the Sino-Korean and Yangtze cratons. *J Metamorph Geol* 22:361–380
- López S, Castro A (2001a) Determination of the fluid-absent solidus and supersolidus phase relationships of MORB-derived amphibolites in the range of 4–14 kbar. *Am Mineral* 86:1396–1403
- López S, Castro A (2001b) Determination of the fluid-absent solidus and supersolidus phase relationships of MORB-derived amphibolites in the range of 4–14 kbar. *Am Miner* 86:1396–1403
- Lucchetti G, Cabella R, Cortesogno L (1990) Pumpellyites and coexisting minerals in different low-grade metamorphic facies of Liguria, Italy. *J Metamorph Geol* 8:539–550
- Lü Z, Zhang L, Du J, Yang X, Tian Z, Xia B (2012) Petrology of HP metamorphic veins in coesite-bearing eclogite from western Tianshan, China: Fluid processes and elemental mobility during exhumation in a cold subduction zone. *Lithos* 136–139:168–186
- Markl G, Bucher K (1997) Eclogites from the early Proterozoic Lofoten Island, N. Norway. *Lithos* 42:15–35
- Maruyama S, Suzuki K, Liou JG (1983) Greenschist-amphibolite transition equilibria at low pressures. *J Petrol* 24:583–604
- Mattinson CG, Zhang RY, Tsujimori T, Liou JG (2004) Epidote-rich talc-kyanite-phengite eclogites, Sulu terrane, eastern China: P-T- f_{O_2} estimates and the significance of the epidote-talc assemblage in eclogite. *Am Miner* 89:1772–1783
- McLelland JM, Selleck BW (2011) Megacrystic Gore Mountain-type garnets in the Adirondack Highlands: age, origin, and tectonic implications. *Geosphere* 7:1194–1208
- Messiga B, Kienast JR, Rebay M, Piccardi P, Tribuzio R (1999) Cr-rich magnesiochloritoid eclogites from the Monviso ophiolites (Western Alps, Italy). *J Metamorph Geol* 17:287–299

- Messiga B, Scambelluri M, Piccardo GB (1995) Chloritoid-bearing assemblages in mafic systems and eclogite-facies hydration of alpine Mg-Al metagabbros (Erro- Tobbio Unit, Ligurian Western Alps). *Eur J Mineral* 7:1149–1167
- Meyre C, Puschign AR (1993) High-pressure metamorphism and deformation at Trescolmen, Adula nappe, Central Alps. *Schweiz Mineral Petrogr Mitt* 73:277–283
- Michell RJ, Johnson TE, Evans K, Gupta S, Clark Ch (2019) Controls on the scales of equilibrium during granulite facies metamorphism. *J Metamorph Geol* 39:519–540
- Miller WJ (1938) Genesis of certain Adirondack garnet deposits. *Am Mineral: J Earth Planet Mater* 23:399–408
- Mongkoltip P, Ashworth JR (1986) Amphibolitization of metagabbros in the Scottish Highlands. *J Metamorph Geol* 4:261–283
- Nakamura D (2003) Stability of phengite and biotite in eclogites and characteristics of biotite- or orthopyroxene-bearing eclogites. *Contrib Miner Petrol* 145:550–567
- Neuhoff PS, Fridriksson T, Arnórsson S, Bird DK (1999) Porosity evolution and mineral paragenesis during low-grade metamorphism of basaltic lavas at Teigarhorn, eastern Iceland. *Am J Sci* 299:467–501
- Newton RC (1986) Metamorphic temperatures and pressures of Group B and C eclogites. *Geol Soc Am Mem* 164:17–30
- Okay AI (1994) Sapphirine and Ti-clinohumite in ultra-high-pressure garnet-pyroxenite and eclogite from Dabie Shan, China. *Contrib Mineral Petrol* 116:145–155
- Okay AI (2002) Jadeite-chloritoid-glaucophane-lawsonite blueschists in north-west Turkey: unusually high P/T ratios in continental crust. *J Metamorph Geol* 20:757–768
- Patíño Douce AE (1993) Titanium substitution in biotite: an empirical model with applications to thermometry, O₂ and H₂O barometries, and consequences for biotite stability. *Chem Geol* 108:133–162
- Patrick BE, Day HW (1989) Controls on the first appearance of jadeitic pyroxene, northern Diablo Range, California. *J Metamorph Geol* 7:629–639
- Pattison DR (1991) Infiltration-driven dehydration and anatexis in granulite facies metagabbro, Grenville Province, Ontario, Canada. *J Metamorph Geol* 9:315–332
- Pattison DRM (2003) Petrogenetic significance of orthopyroxene-free garnet + clinopyroxene + plagioclase ± quartz-bearing metabasites with respect to the amphibolite and granulite facies. *J Metamorph Geol* 21:21–34
- Platt JP (1993) Exhumation of high-pressure rocks: a review of concepts and processes. *Terra Nova* 5:119–133
- Pognante U, Kienast J-R (1987) Blueschist and eclogite transformations in Fe-Ti gabbros: a case from the western Alps ophiolites. *J Petrol* 28:271–292
- Powell WG, Carmichael DM, Hodgson CJ (1993) Thermobarometry in a sub-greenschist to greenschist transition in metabasites of the Abitibi greenstone belt, Superior Province, Canada. *J Metamorph Geol* 11:165–178
- Raimbourg H, Goffé B, Jolivet L (2007) Garnet reequilibration and growth in the eclogite facies and geodynamical evolution near peak metamorphic conditions. *Contrib Miner Petrol* 153:1–28
- Ravna EK, Andersen TB, Jolivet L, de Capitani C (2010) Cold subduction and the formation of lawsonite eclogite—constraints from prograde evolution of eclogized pillow lava from Corsica. *J Metamorph Geol* 28:381–395
- Rebay G, Powell R (2002) The formation of eclogite facies metatroctolites and a general petrogenetic grid in Na₂O-CaO-FeO-MgO-Al₂O₃-SiO₂-H₂O (NCFMASH). *J Metamorph Geol* 20:813–826
- Root DB, Hacker BR, Gans PB, Ducea MN, Eide EA, Mosenfelder JL (2005) Discrete ultrahigh-pressure domains in the Western Gneiss Region, Norway: implications for formation and exhumation. *J Metamorph Geol* 23:45–62
- Russ-Nabelek C (1989) Isochemical contact metamorphism of mafic schist, Laramie Anorthosite Complex, Wyoming: Amphibole compositions and reactions. *Am Mineral* 74:530–548

- Sanders LS (1988) Plagioclase breakdown and regeneration reactions in Grenville kyanite eclogite at Glenelg, NW Scotland. *Contrib Mineral Petrol* 98:33–39
- Schmidt MW, Vielzeuf D, Auzanneau E (2004) Melting and dissolution of subducting crust at high pressures: the key role of white mica. *Earth Planet Sci Lett* 228:65–84
- Šegvić B, Slovenec D, Altherr R, Babajić E, Mählmann RF, Lugović B (2019) Petrogenesis of high-grade metamorphic soles from the Central Dinaric Ophiolite belt and their significance for the Neotethyan evolution in the Dinarides. *Ofoliti* 44:1–30
- Shibuya T, Kitajima K, Lomiya T, Terabayashi M, Maruyama S (2007) Middle Archean ocean ridge hydrothermal metamorphism and alteration recorded in the Cleaverville area, Pilbara Craton, Western Australia. *J Metamorph Geol* 25:751–767
- Smelik EA, Veblen DR (1989) A five-amphibole assemblage from blueschists in northern Vermont. *Am Mineral* 74:960–964
- Smith DC, Lappin MA (1989) Coesite in the Straumen kyanite-eclogite pod, Norway. *Terra Nova* 1:47–56
- Song SG, Zhang LF, Niu Y, Wei CJ, Liou JG, Shu GM (2007) Eclogite and carpholite-bearing metasedimentary rocks in the North Qilian suture zone, NW China: implications for Early Palaeozoic cold oceanic subduction and water transport into mantle. *J Metamorph Geol* 25:547–563
- Soto JI (1993) PTMAFIC: software for thermobarometry and activity calculations with mafic and ultramafic assemblages. *Am Mineral* 78:840–844
- Spear FS (1980) NaSi ↔ CaAl exchange equilibrium between plagioclase and amphibole: An Empirical Model. *Contrib Mineral Petrol* 72:33–41
- Spear FS (1982) Phase equilibria of amphibolites from the Post Pond Volcanics, Mt. Cube quadrangle Vermont. *J Petrol* 22:383–426
- Springer RK, Day HW, Beiersdorfer RE (1992) Prehnite-pumpellyite to greenschist facies transition, Smartville complex, near Auburn, California. *J Metamorph Geol* 10:147–170
- Starkey RJ, Frost BR (1990) Low-grade metamorphism of the Karmutsen Volcanics, Vancouver Island, British Columbia. *J Petrol* 31:167–195
- Starr PG, Pattison DRM (2019) Equilibrium and disequilibrium processes across the greenschist–amphibolite transition zone in metabasites. *Contrib Miner Petrol* 174:1–53
- Starr PG, Pattison DRM, Ames DE (2019) Mineral assemblages and phase equilibria of metabasites from the prehnite–pumpellyite to amphibolite facies, with the Flin Flon Greenstone Belt (Manitoba) as a type example. *J Metamorph Geol* 38:71–102
- Stowell HH, Tulloch A, Zuluaga CA, Koenig A (2010) Timing and duration of garnet granulite metamorphism in magmatic arc crust, Fiordland, New Zealand. *Chem Geol* 273:91–110
- Stowell HH, Odom Parker K, Gatewood MP, Tulloch A, Koenig A (2014) Temporal links between pluton emplacement, garnet granulite metamorphism, partial melting, and extensional collapse in the lower crust of a Cretaceous magmatic arc, Fiordland New Zealand. *J Metamorph Geol* 32:151–175
- Tamblyn R, Hand M, Kelsey D, Anczkiewicz R, Och D (2019) Subduction and accumulation of lawsonite eclogite and garnet blueschist in eastern Australia. *J Metamorphic Geol* 38:157–182
- Terabayashi M (1993) Compositional evolution in Ca-amphibole in the Karmutsen metabasites, Vancouver Island, British Columbia, Canada. *J Metamorph Geol* 11:677–690
- Thieblemont D, Triboulet C, Godard G (1988) Mineralogy, petrology and P-T-t path of Ca-Na amphibole assemblages, Saint-Martin des Noyers formation, Vendée, France. *J Metamorph Geol* 6:697–716
- Thompson AB, Laird J (2005) Calibrations of modal space for metamorphism of mafic schist. *Am Mineral* 90:843–856
- Thompson JB (1991) Modal space: applications to ultramafic and mafic rocks. *Can Mineral* 29:615–632
- Thompson JB, Laird J, Thompson AB (1983) Reactions in amphibolite, greenschist, and blueschist. *J Petrol* 23:1–27

- Topuz G, Okay AI, Altherr R, Satir M, Schwarz H (2008) Late Cretaceous blueschist facies metamorphism in southern Thrace (Turkey) and its geodynamic implications. *Metamorph Geol* 26:895–913
- Triboulet C, Thiéblemont D, Audren C (1992) The (Na-Ca) amphibole- albite- chlorite- epidote- quartz geothermobarometer in the system S- A- F- M- C- N- H₂O. 2. Applications to metabasic rocks in different metamorphic settings. *J Metamorph Geol* 10:557–566
- Tual L, Möller C, Whitehouse MJ (2018) Tracking the prograde P-T path of Precambrian eclogite using Ti-in quartz and Zr-in-rutile geothermobarometry. *Contrib Mineral Petrol* 173(56):1–15
- Tursi F, Bianco C, Brogi A, Caggianelli A, Prosser G, Ruggieri G, Braschi E (2020) Cold subduction zone in northern Calabria (Italy) revealed by lawsonite-clinopyroxene blueschists. *J Metamorph Geol* 38:451–469
- Wang Q, Zhang L, Song S (2007) p-T condition and phase equilibrium of lawsonite-blueschists in northern Qilian Mountains and its petrologic significance. *Earth Sci Front* 14:157–171
- Wei CJ, Song SG (2008) Chloritoid-glaucophane schist in the north Qilian orogen, NW China: phase equilibria and P-T path from garnet zonation. *J Metamorph Geol* 26:301–316
- Wei CJ, Yang Y, Su XL, Song SG, Zhang LF (2009) Metamorphic evolution of low-T eclogite from the North Qilian orogen, NW China: evidence from petrology and calculated phase equilibria in the system NCKFMASHO. *J Metamorph Geol* 27:55–70
- Wolke C, Truckenbrodt J, Johannes W (1995) Beginning of dehydration-melting in amphibolites at $P \leq 10$ kbar. *Eur J Mineral* 7:273
- Xia B, Brown M, Zhang L (2020) P-T evolution and tectonic significance of lawsonite-bearing schists from the eastern segment of the southwestern Tianshan, China. *J Metamorph Geol* 38:935–962
- Yang J-J, Powell R (2006) Calculated phase relations in the system Na₂O-CaO-K₂O-FeO-MgO-Al₂O₃-SiO₂-H₂O with applications to UHP eclogites and whiteschists. *J Petrol* 47:2047–2071
- Zack T, Luvizottow GL (2006) Application of rutile thermometry to eclogites. *Mineral Petrol* 88:69–85
- Zen E-an (1961) The zeolite facies: an interpretation. *Am J Sci* 259:401–409
- Zhang G, Ellis DJ, Christy AG, Zhang L, Niu Y, Song S (2009) UHP metamorphic evolution of coesite-bearing eclogite from the Yuka terrane, North Qaidam UHPM belt, NW China. *Eur J Mineral* 21:1287–1300
- Zhang G, Song S, Zhang L, Niu Y (2008) The subducted oceanic crust within continental-type UHP metamorphic belt in the North Qaidam, NW China: evidence from petrology, geochemistry and geochronology. *Lithos* 104:99–118
- Zhang L, Song S, Liou JG, Ai Y, Li X (2005) Relict coesite exsolution in omphacite from Western Tianshan eclogites, China. *Am Miner* 90:1092–1099